Role of Na-H Exchangers and Vacuolar H^+ Pumps in Intracellular pH Regulation in Neonatal Rat Osteoclasts

JAN H. RAVESLOOT,*‡ THOMAS EISEN,* ROLAND BARON,‡ and WALTER F. BORON*

From the *Department of Cellular and Molecular Physiology, and ‡Departments of Orthopaedics and Cell Biology, Yale University School of Medicine, New Haven, Connecticut 06510

ABSTRACT Osteoclasts resorb bone by pumping of H^+ into a compartment between the cell and the bone surface. Intracellular pH (pH_i) homeostasis requires that this acid extrusion, mediated by a vacuolar-type H^+ ATPase, be complemented by other acid-base transporters. We investigated acid-extrusion mechanisms of single, freshly isolated, neonatal rat osteoclasts. Cells adherent to glass coverslips were studied in the nominal absence of CO_2/HCO_3^-, using the pH-sensitive dye BCECF and a digital imaging system. Initial pH_i averaged 7.31 and was uniform throughout individual cells. Intrinsic buffering power (β_I) decreased curvilinearly from ~25 mM at pH_i = 6.4 to ~6.0 mM at pH_i = 7.4. In all polygonally shaped osteoclasts, and ~60% of round osteoclasts (~20% of total), pH_i recovery from acid loads was mediated exclusively by Na-H exchange. In these pattern-1 cells, pH_i recovery was 95% complete within 200 s, and was blocked by removing Na^+, or by applying 1 mM amiloride, 50 μM ethylisopropylamiloride (EIPA), or 50 μM hexamethyleneamiloride (HMA). The apparent $K_{1/2}$ for HMA ($[Na^+]_o$ = 150 mM) was 49 nM, and the apparent $K_{1/2}$ for Na^+ was 45 mM. Na-H exchange, corrected for amiloride-insensitive fluxes, was half maximal at pH_i 6.73, with an apparent Hill coefficient for intracellular H^+ of 2.9. Maximal Na-H exchange averaged 741 μM/s. In the remaining ~40% of round osteoclasts (pattern-2 cells), pH_i recovery from acid loads was brisk even in the absence of Na^+ or presence of amiloride. This Na^+-independent pH_i recovery was blocked by 7-chloro-4-nitrobenz-2-oxa-1,3-diazol (NBD-Cl), a vacuolar-type H^+ pump inhibitor. Corrected for NBD-Cl insensitive fluxes, H^+ pump fluxes decreased approximately linearly from 96 at pH_i 6.8 to 11 μM/s at pH_i 7.45. In ~45% of pattern-2 cells, Na^+ readdition elicited a further pH_i recovery, suggesting that H^+ pumps and Na-H exchangers can exist

Address correspondence to W. F. Boron at Department of Cellular and Molecular Physiology, Yale University School of Medicine, 333 Cedar Street, New Haven, CT 06510.

Dr. Ravesloot's present address is Department of Physiology, University of Amsterdam, Meibergdreef 15, 1105 AZ Amsterdam, The Netherlands.

Dr. Eisen's present address is Department of Internal Medicine, Yale University School of Medicine, 333 Cedar Street, New Haven, CT 06510.

J. GEN. PHYSIOL. © The Rockefeller University Press · 0022-1295/95/02/0177/32 $2.00
Volume 105 February 1995 177–208

simultaneously. We conclude that, under the conditions of our study, most neonatal rat osteoclasts express Na-H exchangers that are probably of the ubiquitous basolateral subtype. Some cells express vacuolar-type H^+ pumps in their plasma membrane, as do active osteoclasts in situ.

INTRODUCTION

Physiological bone resorption is required for the development and growth of the skeleton, for its remodeling throughout life, and for supplying free Ca^{2+} to the systemic fluids. This process, which involves the degradation of a mineralized extracellular matrix, is performed by the osteoclast, a large, multinucleated cell derived from the hematopoietic bone marrow. To perform its function, the osteoclast attaches firmly to the bone surface, forming a specialized circumferential region, the "sealing zone," where actin and other cytoskeletal proteins accumulate in the cytoplasm and integrin receptors are present in the plasma membrane. This zone of attachment surrounds a highly folded region of the plasma membrane, termed the "ruffled border," which directly faces the bone surface. The osteoclast actively acidifies and secretes enzymes into the bone-resorbing compartment, which is surrounded by the sealing zone and lies between the ruffled-border membrane and the bone surface. This leads to the formation of a resorption cavity (Baron, Neff, Louvard, and Courtoy, 1985; Baron, 1989). Carbonic anhydrase is highly expressed in the osteoclast cytosol (Gay, Ito, and Schraer, 1983), and presumably plays a key role in generating H^+ from CO_2. The protons thus formed are translocated across the plasma membrane at the ruffled border, which is very highly enriched in vacuolar-type H^+ pumps (Blair, Teitelbaum, Ghiselli, and Gluck, 1989; Vaananen, Karhukorpi, Sundquist, Wallmark, Roininen, Hentunen, Tuukkanen, and Lakkakorpi, 1990; Chatterjee, Chakraborty, Leit, Neff, Jamsa-Kellokumpu, Fuchs, and Baron, 1992). Hence, although the osteoclast is not part of an epithelium, it is a polarized cell. It has an apical pole, the ruffled border, where secretion and H^+ transport occur, and a basolateral domain, where high numbers of Na-K pumps are present (Baron, Neff, Roy, Boisvert, and Kaplan, 1986).

Regulation of the intracellular pH (pH_i) may be expected to be of critical importance for resorbing osteoclasts. If unopposed, the extrusion of large amounts of acid would cause pH_i to rise, with detrimental effects for many cellular processes. Therefore, osteoclasts may be expected to possess various acid-base transporters that operate simultaneously with the proton pumps, and thereby keep pH_i within a favorable range. Consistent with this view are the observations that blockade of Na-H exchange or Cl-HCO_3 exchange impairs the osteoclast's ability to form resorption pits in bone slices (Hall and Chambers, 1989, 1990; Baron, Bartkiewicz, Chakraborty, Chatterjee, Fabricant, Hernando, Horne, Lomri, Neff, Ravesloot, and Su, 1992). Direct measurements of pH_i confirmed the presence of anion exchangers in avian osteoclasts (Teti, Blair, Teitelbaum, Kahn, Koziol, Konsek, Zambonin-Zallone, and Schlesinger, 1989).

Despite their importance for bone resorption, not much is known about the roles played in pH_i regulation by Na-H exchangers or other transporters that defend avian or mammalian osteoclasts against acid loads. The main focus of the present study was

to identify the mechanisms by which osteoclasts, freshly isolated from neonatal rats and attached to glass coverslips, defend themselves against acute cytoplasmic acid loads. By conducting the experiments in the nominal absence of CO_2/HCO_3^-, we minimized the contribution of HCO_3^--dependent acid-base transporters to pH_i regulation. Because osteoclasts cannot be isolated from endosteal bone surfaces in sufficient amounts and with sufficient purity to allow population studies, we used the digital imaging of the fluorescent pH-sensitive dye BCECF to monitor pH_i in single cells. We found that most if not all osteoclasts express Na-H exchange activity that is highly sensitive to inhibition by hexamethyleneamiloride. This suggests that the exchangers may be of the ubiquitous, basolateral subtype. In addition, a distinct subpopulation of osteoclasts possess an Na^+-independent, amiloride-insensitive acid-extrusion mechanism that is blocked by 7-chloro-4-nitrobenz-2-oxa-1,3-diazol (NBD-Cl), an inhibitor of vacuolar-type proton pumps. Finally, we found that intrinsic intracellular buffering power is a curvilinear function of pH_i, decreasing with increasing pH_i values.

Portions of this work have been presented elsewhere in abstract form (Eisen, Su, Baron, and Boron, 1991; Ravesloot, Boron, and Baron, 1992).

MATERIALS AND METHODS

Cell Isolation

Osteoclasts were isolated from the long bones of 1–5-d old neonatal Wistar rats essentially as described by Boyde, Ali, and Jones, (1984) and Chambers, Reveli, Fuller, and Athanasou, (1984). Tibiae, femora and humeri were removed and placed in culture medium, which consisted of the alpha modification of minimal essential medium (α-MEM, Sigma Chemical Co., St. Louis, MO) supplemented with 10% heat-inactivated fetal-calf serum (Sigma Chemical Co.) and antibiotics (penicillin and streptomycin, Sigma Chemical Co.). After shredding the bones, we dispersed the cells by passaging the bone fragments gently through a Pasteur pipette. The resulting cell suspension, usually 4 ml, was plated on glass coverslips. Before the cells were plated on them, the coverslips were exposed to serum for 40 min or, in a few experiments, coated with type-I collagen (Sigma Chemical Co.) to improve adherence of the cells. Cells were allowed to sediment for 40–60 min in a 5% CO_2 incubator at 37°C. Finally, the coverslips were washed with α-MEM to remove nonadherent cells, and incubated in culture medium until use (with a maximum delay of 10 h).

Solutions

Table I lists the composition of the solutions used. In some experiments, flame photometry was used to confirm the Na^+ concentration of the solutions. Using a vapor-pressure osmometer (Wescor Inc., Logan, UT), we verified that the osmolality of the solutions was between 290 and 310 mOsm/kg H_2O. 2′,7′-bis-2-carboxyethyl)-5(and-6)carboxyfluorescein/tetraacetoxymethyl ester (BCECF-AM, Molecular Probes, Inc., Eugene, OR) was prepared as a 10-mM stock solution in dimethylsulfoxide (DMSO, Sigma Chemical Co.). Nigericin (Sigma Chemical Co.) was prepared as a 10-mM stock solution in ethanol. The amiloride analogues ethylisopropyl-amiloride (EIPA), and hexamethyleneamiloride (HMA) were purchased from E. J. Cragoe, Jr. (Nacogdoches, TX) and were prepared as a 50-mM stock solution in DMSO. 7-chloro-4-nitrobenz-2-oxa-1,3-diazol (NBD-Cl, Sigma Chemical Co.) was prepared as a 100-mM stock in DMSO before each experiment.

Fluorescence Experiments

Cells were loaded with the acetoxymethyl ester of the pH sensitive dye BCECF (BCECF-AM). To this end the coverslips were placed in a HEPES-buffered solution (solution 1, Table I) containing 10–15 μM of BCECF-AM at 37°C for 20–40 min in an air-gassed incubator. The coverslip was then placed and secured in a chamber on the stage of a Zeiss IM35 inverted microscope equipped with differential interference contrast (DIC) microscopy optics and apparatus for epiillumination. The chamber was continuously superfused with prewarmed solutions to give a bath temperature of 37°C. This temperature was monitored continuously by a thermistor. The chamber had two inlets connected to the tubing of two separate solution delivery systems. One system was used exclusively for the delivery of the nigericin containing

TABLE I

*Solutions**

Solute	Solution 1 Standard HEPES	Solution 2 NH_4^+	Solution 3 High-K^+ Nigericin	Solution 4 15.5 mM Na^+	Solution 5 0 Na^+	Solution 6 0 Na^+
Na^+	142.8	122.8	0	15.5	0	0
NH_4^+	0	20.0	0	0	0	40.0
$NMDG^+$	0	0	32.8	129.5	145	102.8
K^+	5.0	5.0	100.0	5.0	5.0	5.0
Ca^{++}	2.0	2.0	2.0	2.0	2.0	2.0
Mg^{++}	2.4	2.4	2.4	2.4	2.4	2.4
mEq/l (+)	152.2	152.2	137.2	154.4	154.4	152.2
Cl^-	132.0	132.0	123.9	134.2	134.2	132.0
$H_2PO_4^-$	0.4	0.4	0.8	0.4	0.4	0.4
$HPO_4^=$	3.2	3.2	2.4	3.2	3.2	3.2
$HEPES^-$	14.2	14.2	7.7	14.2	14.2	14.2
$SO_4^=$	2.4	2.4	2.4	2.4	2.4	2.4
mEq/l (−)	152.2	152.2	137.2	154.4	154.4	152.2
Glucose	10.5	10.5	10.5	10.5	10.5	10.5
$HEPES^0$	17.8	17.8	24.3	17.8	17.8	17.8
Mannitol	0	0	25.0	0	0	0
mM (neutral)	28.3	28.3	59.8	28.3	28.3	28.3
pH	7.4	7.4	7.0	7.4	7.4	7.4

*Solutions 1 and 2 were titrated with NaOH. For solutions 3–6, the free base NMDG was titrated with HCl. All titrations were done at 37°C. The concentrations of the HEPES-free acid ($HEPES^0$) and its conjugate weak base ($HEPES^-$) were computed assuming a pK of 7.5. The concentrations of inorganic phosphate species were computed assuming a pK of 6.8.

high-K^+ solutions (solution 3), the second one for all other solutions. Using DIC optics, osteoclasts were easily identified among the many mononuclear bone marrow cells by their shape, size and many nuclei. Routinely, two DIC images of the osteoclast were stored, one before and one after the experiment. The entire microscopic field, including the osteoclast selected for fluorescence experiments, was alternately excited with light of wavelengths of 490 and 440 nm and the light emitted by the dye of wavelength of 530 nm was imaged for both exciting wavelengths (I_{490} and I_{440}). The light source in the fluorescence experiments was a 100-W Tungsten halogen lamp. The arrangement of dichroic mirrors, filters and computer-controlled shutters, used to generate the 490- and 440-nm light, is described elsewhere (Boyarsky, Ganz, Sterzel, and Boron, 1988). To limit both photobleaching of the dye and

photodynamic damage of the cells, illumination was limited to 450 ms for the 490-nm light, followed immediately by 450 ms for the 440-nm light. This pair of excitations was repeated at intervals varying from 5–20 s; between the excitations, the cells were in the dark. The emitted light was collected through a 63×/1.25 NA oil-immersion objective. The light passes through a 510-nm long-pass dichroic mirror and a 530-nm long-pass filter located in the filter cube underneath the turret of the microscope. The light was then amplified by an image intensifier (KS-1381 intensifier, Video Scope International, Ltd, Washington, DC), before it was captured with a charged-coupled device camera (CCD 72, Dage M.T.I., Michigan City, IN). Each cycle of excitations had the following protocol: the shutters gating the 490-nm light were opened. After a delay of 100 ms, to allow for stabilization of the signal, we collected, digitized and averaged eight successive TV frames using an image processor (Itex 151, Imaging Technology Inc, Woburn, MA). After storage of the averaged image, the 490-nm shutters were closed, the 440-nm shutters were opened after a 166-ms delay and an averaged 440-nm image was obtained in the same way. No background subtraction was performed (see below). The averaged images were transferred in real time to a Compaq 386/20 personal computer with 300-Mb storage capacity. At the conclusion of each experiment, the data were transferred to a 2.1-Gb digital tape (Emerald Systems, San Diego, CA) for later analysis. The DOS-based computer software used to control the data acquisition, as well as the Windows-based software used to perform the off-line analysis, was developed in our laboratory. For the analysis, we used a mouse to outline areas of interest, which could be the entire cell or portions thereof. Typically, we grouped together and analyzed the pixels that corresponded to the nuclei as well as the cytoplasm between or surrounded by the nuclei. The sum of the I_{490} values of the pixels in the area of interest was divided by the sum of the corresponding I_{440} values. The resulting ratio is strongly dependent on pH_i but relatively insensitive to other factors, such as dye concentration.

Calculation of Intracellular pH

Conversion of the I_{490}/I_{440} ratios to pH_i values was done according the high-K^+/nigericin technique of Thomas, Buschbaum, Zimniak, and Racker (1979), as modified by Boyarsky et al. (1988). At the end of each experiment (see Fig. 6 *C*), the osteoclast was exposed to a high-K^+ solution (solution 3), titrated to pH 7.00, to which 10 μM nigericin was added. The potential limitations of this approach are discussed elsewhere (Chaillet and Boron, 1985). The I_{490}/I_{440} ratios of the entire experiment were normalized by dividing them by the I_{490}/I_{440} ratio corresponding to pH 7.00. pH_i was then calculated using the following equation (Boyarsky et al., 1988):

$$\frac{I_{490}/I_{440}}{(I_{490}/I_{440})_{pH=7}} = 1 + b\left[\frac{1}{1 + 10^{(pK-pH)}} - \frac{1}{1 + 10^{(pK-7)}}\right].$$

The values of pK and b were determined from experiments in which osteoclasts were exposed to a series of 2–11 10 μM nigericin-containing solutions at different pH, always including pH 7.00. An example of such an experiment is shown in Fig. 1 *A*. Fig. 1 *B* shows the values of $(I_{490}/I_{440})/(I_{490}/I_{440})_{pH=7}$ as a function of pH_i obtained from a total of 75 osteoclasts. The data were fitted by the above equation, which forces the best-fit curve to pass through unity at pH_i = 7.00, using a nonlinear least-squares method. The best values were pK = 7.34 ± 0.02 (SD) and b = 1.80 ± 0.02 (SD). The background fluorescence always was <1% of the dye signal. The average background fluorescence intensity as determined in 13 cells was 0.321 ± 0.039% (n = 40) of the I_{440} signal and 0.318 ± 0.043% (n = 40) of the I_{490} signal as recorded at the end of the nigericin calibration procedure. For these reasons the background fluorescence was not subtracted from the I_{490} and I_{440} values.

Determination of the Intrinsic Buffering, β_I

Acid-loaded osteoclasts were exposed to a series of nominally Na^+-free solutions that contained 20, 10, 5, 2.5, 1, 0.5, and 0 mM total ammonium (see Fig. 7 *A*), following the approach of Boyarsky et al. (1988). NH_3/NH_4^+-containing solutions were prepared by mixing solution 5 and solution 6 (Table I). With each stepwise decrease in $[NH_3/NH_4^+]_o$, the amount of protons delivered to the cytoplasm ($\Delta[acid]_i$) was considered equal to the resultant change in $[NH_4^+]_i$. If it is assumed that the $[NH_3]_i$ equals $[NH_3]_o$, and that the pK_a governing the NH_3/NH_4^+ equilibrium (8.90 at 37°C) is the same in the cytoplasm as in the extracellular fluid, $[NH_4^+]_i$ can be calculated from the observed pH_i. ΔpH_i was taken as the change in pH_i produced by the stepwise decrease in $[NH_3/NH_4^+]_o$. β_I was then calculated as $-\Delta[acid]_i/\Delta pH_i$ (Roos and Boron, 1981). β_I was assigned to the mean of the two pH_i values used for its calculation.

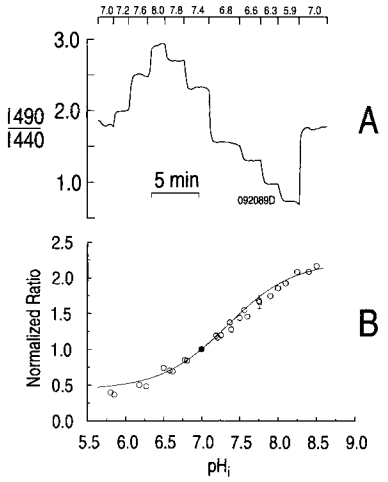

FIGURE 1. Multipoint intracellular calibration of the pH-sensitive dye BCECF present in the cytoplasm of neonatal rat osteoclasts. (*A*) Typical example of the changes of the I_{490}/I_{440} ratio observed in an osteoclast exposed to a series of high-K^+/10-μM nigericin solutions (solution 3) titrated to the pH values indicated. Normalized I_{490}/I_{440} ratios are obtained by dividing the raw I_{490}/I_{440} ratio by the raw ratio corresponding to a pH_i of 7.00. Note that the I_{490}/I_{440} ratios corresponding to pH_i 7.00 at the beginning and the end of this 24-min experiment are virtually identical. (*B*) Plot of the mean value of the normalized ratios versus pH_i. The figure summarizes data obtained from 75 experiments similar to that shown in *A*: each symbol represents at least three observations. The curve through the points is the result of a nonlinear least-squares fit. From the fitted curve, the pH_i values corresponding to normalized ratios of all subsequent experiments were determined. Therefore, all experiments were concluded by exposing the osteoclasts to high-K^+/nigericin solution titrated at pH = 7.00 (see also Fig. 6 *C*). Vertical bars represent the SEM, and are omitted if the SEM does not exceed the symbol radius by at least 25%. The filled symbol marks the position corresponding to a normalized ratio of 1.0 at pH_i = 7.00.

Data Analysis

First to fourth order polynomial functions were fitted to the pH_i transients using least-squares fitting methods. The rate of pH_i change per unit time (dpH_i/dt) was calculated by differentiating the polynomial function at any selected pH_i. The software package used for this purpose was developed in our laboratory. Statistical analysis as well as some of the nonlinear least-squares fits (Hill equation, buffering power vs pH of monoprotic weak acid) were performed with the software package "Systat" (Systat Inc., Evanston, IL). Two sets of data were considered significantly different, if the *P* value of the (paired) *t* test was <0.05. Results are given as mean ± SEM, with the number of cells (*n*) from which it was calculated, unless stated otherwise.

RESULTS

Cell Morphology

Under our conditions for isolating and culturing osteoclasts, we recognized two major types of cell morphology. The cells of the first group, which represented the majority, were well spread, and displayed irregularly shaped cytoplasmic extensions that projected from an elongated and/or polygonal cell body. A digital fluorescence image of such a cell, excited at 440 nm, is shown in Fig. 2 *A*. Sometimes the extension (apron) was devoid of subcellular structures that could be resolved with DIC microscopy. The nuclei of these cells tended to be arranged linearly, and the cytoplasm had a granular appearance. These cells often rearranged the shape of their extensions over the course of an experiment (15–40 min). The cells of the second group had a round shape, no cytoplasmic extensions, and the nuclei were clustered in the center (see Fig. 2 *B*). These cells, too, were well spread. In general, the aprons of these cells surrounded the cytoplasm completely. We used both types of osteoclasts in our experiments.

Dye Behavior

In examining individual I_{490} and I_{440} images of BCECF-loaded osteoclasts, we generally observed three regions with different, though uniform, fluorescence intensities. The highest fluorescence intensity was found over the nuclei. The fluorescence intensity was usually lower in the perinuclear region, which corresponded to the granular, organelle-containing part of the cytoplasm. Finally, the fluorescence intensity was lowest, and in fact often negligible, in the apron. The regional differences in intensities, however, did not reflect regional pH_i differences, inasmuch as pseudo-images, constructed from the predominantly pH_i-sensitive I_{490}/I_{440} ratios, showed no important regional variation. Similarly, pH_i values averaged over the nuclei were virtually identical to those measured over the perinuclear region in all cells tested.

Distribution of Initial pH_i Values

We found that the distribution of initial pH_i values for osteoclasts studied in the nominal absence of CO_2/HCO_3^- was approximately Gaussian (not shown), with a slight skewness toward alkaline pH_i values. The median value, 7.27, differs only slightly from the mean initial pH_i of 7.31 ± 0.01 ($n = 245$). A relatively small number of osteoclasts (26 or 11% of the total) had initial pH_i values > 7.6, contributing to the skewness. Monitoring pH_i for 15–35 min revealed a slow decline with time; the rate of the decline ranged between 0 and -1.0×10^{-4} pH/s, and averaged $-0.71 \pm 0.29 \times 10^{-4}$ ($n = 7$).

Osteoclasts Recover from Acute Acid Loads

To test for the presence of acid-extruding transporters, we acid loaded osteoclasts in the nominal absence of CO_2/HCO_3^- by means of an NH_4^+ prepulse. To this end, we exposed osteoclasts to a HEPES-buffered solution in which 20 mM NaCl was replaced by 20 mM NH_4Cl. At a pH of 7.4, this solution contains ~ 0.6 mM NH_3. As shown in Fig. 3, the application of NH_3/NH_4^+ causes a rapid increase in pH_i, due to

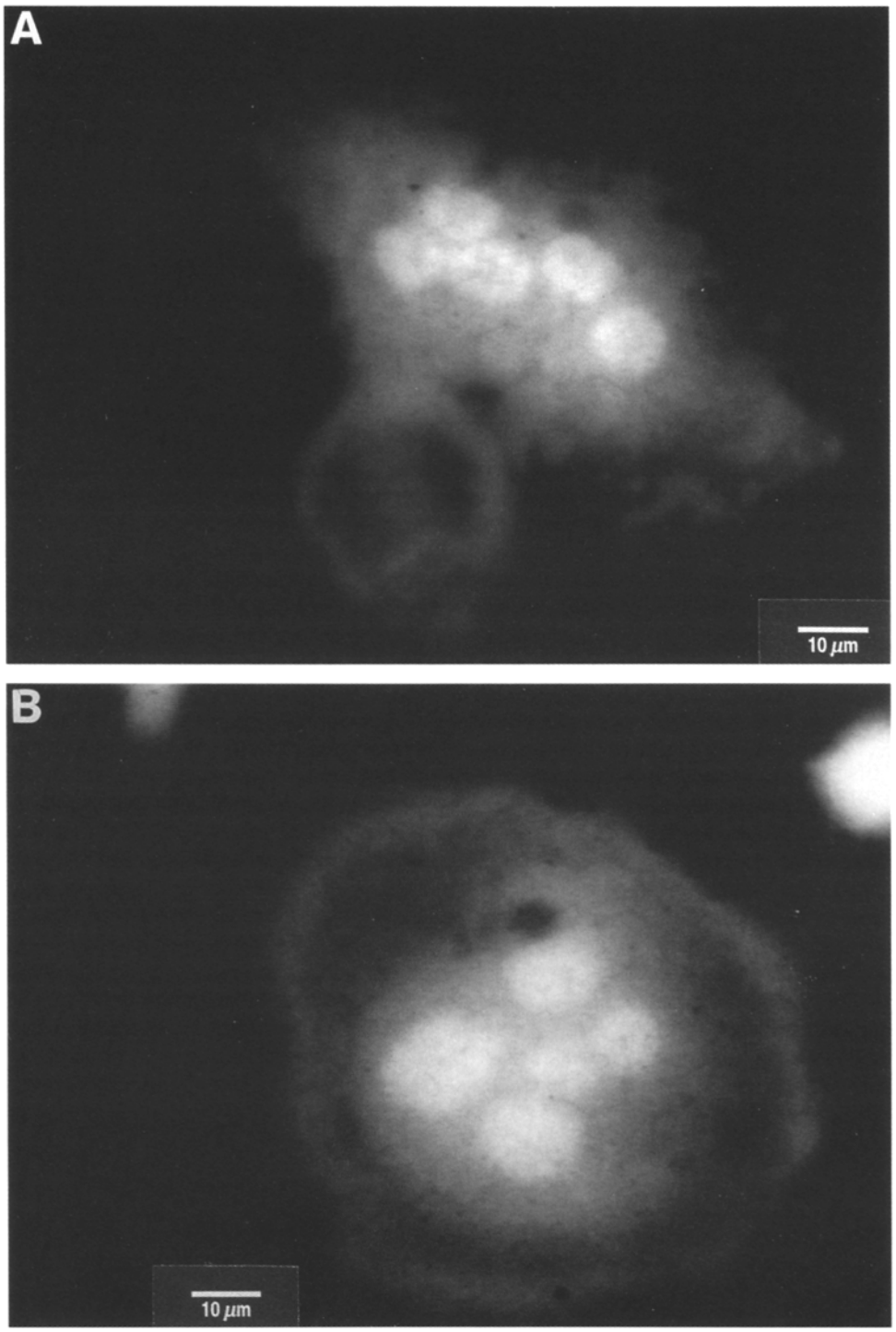

FIGURE 2. Digital fluorescence images of freshly isolated osteoclasts. (*A*) A polygonally shaped cell. (*B*) A round cell. Intracellular BCECF was excited at 440 nm.

the influx of NH_3 and its subsequent association with H^+ to form NH_4^+. The slow pH_i decrease during the subsequent plateau phase is the result of acidifying processes, such as the entry of NH_4^+, a fraction of which will dissociate into NH_3 and H^+. After the extracellular NH_3/NH_4^+ is removed, the resulting efflux of NH_3 causes dissociation of all intracellular NH_4^+. At the end of this acidification phase, the cell is virtually free of NH_3/NH_4^+, and the protons thus generated cause pH_i to fall far below the initial value. The amount of acid loaded into the cell, which is a function of the duration of the plateau-phase NH_3/NH_4^+ exposure, determines the degree of the cytoplasmic acidification. In a total of 51 experiments with an 85-s plateau-phase, pH_i fell during the acidification phase by an average of 0.43 ± 0.02 below the initial pH_i.

In other cells, the intracellular acid load produced by an NH_3/NH_4^+ prepulse stimulates acid-base transporters in the plasma membrane to extrude acid, thereby returning pH_i toward normal (see Boron, 1983). This also was the case for all the 51 osteoclasts we studied. As shown in Fig. 3, we found that the rate of pH_i recovery (dpH_i/dt) was pH_i dependent. It was maximal at, or close to, the lowest pH_i value, and decreased with increasing pH_i. In 15 osteoclasts, in which the cytoplasm was acidified to values between 6.70 and 6.85 (mean: 6.79 ± 0.01), the mean dpH_i/dt was $36 \pm 4 \times 10^{-4}$ pH/s at a pH_i of 6.85. This mean dpH_i/dt will be referred to as the

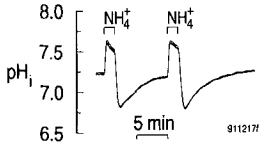

FIGURE 3. pH_i in a rat osteoclast recovers from an acute acid load. The cell was exposed for 85 s to a solution containing 20 mM NH_3/NH_4^+ (solution 2). Subsequently, the cell was switched to the standard HEPES-buffered saline (solution 1). Five pH_i tracings, recorded in five different regions of the same cell are superimposed. No important regional differences in pH_i can be observed.

mean pH_i recovery rate under "control conditions." The time necessary for pH_i to reach the midpoint (6.96 ± 0.02) between the lowest and final pH_i values was 65 ± 8 s. At this midpoint, dpH_i/dt had decreased to $24 \pm 3 \times 10^{-4}$ pH/s. The time necessary for pH_i to reach 95% of its final value was 190 ± 20 s. The mean final pH_i for all 51 osteoclasts examined was 7.19 ± 0.02, which is 0.085 lower than the average initial pH_i observed in this group of osteoclasts ($P < 10^{-7}$).

In a few experiments, the osteoclast was submitted to a second 85-s NH_3/NH_4^+ prepulse after it had recovered from the first. As illustrated in Fig. 3, the recovery of pH_i from the second acute acid load was similar to that observed for the first. On average (see Table II), neither the minimum pH_i value after washout of the NH_3/NH_4^+ prepulse, the magnitude of this acidification, the maximal dpH_i/dt value during the pH_i recovery, the dpH_i/dt value determined at a pH_i of 6.90, nor the final pH_i value reached after the pH_i recovery were significantly different between the first and second pH_i recoveries.

Recovery from Acid Loads, under Conditions of Reduced Extracellular [Na^+], Follows One of Two Patterns

In the nominal absence of CO_2/HCO_3^-, the recovery of pH_i from an acid load in most mammalian cells is mediated by Na-H exchange. To test whether osteoclasts express

TABLE II

*Comparison of Paired NH_3/NH_4^+ Pulses under Control Conditions**

Parameter	First pulse	Second pulse	n	Significance
Minimum pH_i	6.78 ± 0.04	6.71 ± 0.05	9	NS
Initial vs minimum pH_i	−0.38 ± 0.03	−0.38 ± 0.04	9	NS
Max dpH_i/dt (10^{-4} pH/s)	26 ± 6.4	28 ± 3.6	9	NS
pH_i at max dpH_i/dt	6.82 ± 0.04	6.74 ± 0.07	9	NS
dpH_i/dt at pH_i 6.90 (10^{-4} pH/s)	17 ± 5	13 ± 3	7	NS
Final pH_i	7.10 ± 0.06	7.11 ± 0.07	8	NS

*The experiments followed the protocol of Fig. 3. Minimum pH_i is the lowest pH_i achieved after washout of NH_3/NH_4^+. Initial vs minimum pH_i is the difference between the pH_i value prevailing before application of the NH_3/NH_4^+ and the minimum pH_i. Max dpH_i/dt is the maximal rate of pH_i recovery, measured at pH_i at max dpH_i/dt; this pH_i is slightly higher than the minimum pH_i. dpH_i/dt at pH_i 6.9 is the pH_i recovery rate measured at pH_i of 6.9. Final pH_i is value prevailing after recovery of pH_i from the acid load was complete. n is the number of observations. Significance was judged on the basis of paired t tests, comparing values for the first and second pulses.

Na-H exchangers, we used three experimental protocols to examine the effects of lowering of the extracellular Na^+ concentration ($[Na^+]_o$) on the rate of pH_i recovery from acid loads. In the first, shown in Fig. 4 *A*, we twice acid loaded the osteoclast by means of a 85-s NH_4^+-prepulse, as described in the preceding paragraph. The pH_i recovery from the first acid load, under control conditions, had a maximal rate of

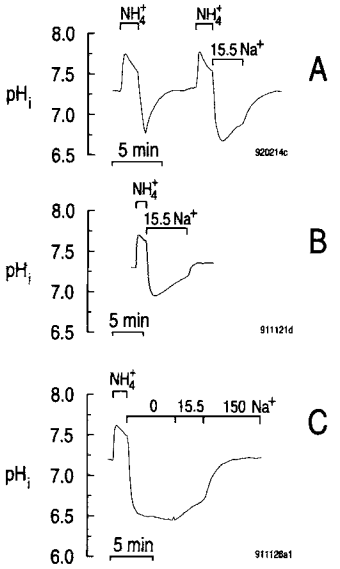

FIGURE 4. Recovery from acid loads in pattern-1 cells is Na^+ dependent. (*A*) Protocol 1. The osteoclast was twice exposed for 85 s to 20 mM NH_3/NH_4^+ (solution 2). After the first acid load, the cell was exposed to the standard HEPES-buffered saline (solution 1) and allowed to recover from the acid load. After the second, the osteoclast was exposed to a solution containing only 15.5 mM Na^+ (solution 4); this decreased the rate of pH_i recovery by 72%. Restoring $[Na^+]_o$ to 150 mM (solution 1) caused dpH_i/dt to increase to control values. (*B*) Protocol 2. The osteoclast was acid loaded by an 85-s exposure to 20 mM NH_3/NH_4^+ (solution 2). Subsequently, the cell was exposed to solutions containing 15.5 mM Na^+ (solution 4) and 150 mM Na^+ (solution 1). In this cell, the rate of pH_i recovery, relative to that in 150 mM Na^+, was reduced 82% in the presence of 15.5 mM Na^+. (*C*) Protocol 3. The osteoclast was exposed for 85 s to 20 mM NH_3/NH_4^+ (solution 2). Subsequently, the external solutions were switched to ones containing nominally no Na^+ (solution 5), 15.5 mM Na^+ (solution 4) and 150 mM Na^+ (solution 1). No recovery from the acid load was observed in the Na^+-free solution, whereas in the presence of 15.5 mM Na^+ the rate of recovery was 84% lower than that observed in the presence of 150 mM Na^+.

47 ± 6.3 × 10^{-4} pH/s at an average pH_i of 6.83 ± 0.04 (n = 13). The pH_i recovery from the second acid load, under conditions in which $[Na^+]_o$ had been reduced to 15.5 mM, followed one of two patterns. In five of the 13 cells, which we define as pattern-2 cells, pH_i recovered rapidly in the presence of 15.5 mM Na^+, with an average dpH_i/dt 35 ± 4.6 × 10^{-4} pH/s determined at a mean pH_i of 7.08 ± 0.06. This was only modestly slower than the matched pH_i recovery in these same cells under control $[Na^+]_o$ conditions, 54 ± 12 × 10^{-4} pH/s (mean pH_i = 6.83 ± 0.06; n = 5). These pattern-2 cells, which appear to have substantial Na^+-independent acid-extrusion activity, are discussed at the end of Results. In the other eight cells, which appeared to lack such an acid extruder, the pH_i recovery was very slow when $[Na^+]_o$ was 15.5 mM, as typified by the experiment shown in Fig. 4 *A*. Subsequently raising $[Na^+]_o$ to 150 mM caused pH_i to recover rapidly, consistent with the presence of a Na-H exchanger. As summarized in Table III (protocol 1), the mean maximal

TABLE III

*Effect of Low $[Na^+]_o$ on Rates of pH_i Recovery from Acid Loads Applied by an NH_3/NH_4^+ Prepulse**

$[Na^+]_o$	Protocol 1 (n = 8)		Protocol 2 (n = 10)		Protocol 3 (n = 21)	
	dpH_i/dt	pH_i at dpH_i/dt	dpH_i/dt	pH_i at dpH_i/dt	dpH_i/dt	pH_i at dpH_i/dt
mM	*10^{-4} pH/s*		*10^{-4} pH/s*		*10^{-4} pH/s*	
0	—	—	—	—	−1.3 ± 0.6	6.56 ± 0.02‡
15.5	13 ± 1	6.71 ± 0.03	6.3 ± 1.1	6.86 ± 0.06§	31 ± 5	6.66 ± 0.02
150	40 ± 5	6.88 ± 0.03	46 ± 9	7.01 ± 0.06	56 ± 5	6.79 ± 0.02

*In Protocol 1 (Fig. 4 *A*), the osteoclast was twice acid loaded via NH_3/NH_4^+ prepulses. After the first acid load, the NH_3/NH_4^+ was washed out into 150 mM Na^+ (not summarized here). After the second, the NH_3/NH_4^+ was washed out into a solution containing 15.5 mM Na^+, which was then switched to one containing 150 mM Na^+. In Protocol 2 (Fig. 4 *B*), the osteoclast was acid loaded only once. The NH_3/NH_4^+ was washed out into a solution containing 15.5 mM Na^+; this was then switched to one containing 150 mM Na. In Protocol 3 (Fig. 4 *C*), the osteoclast was acid loaded only once. The NH_3/NH_4^+ was washed out into a Na^+-free solution, which was switched to ones containing 15.5 mM and then 150 mM Na^+.

‡This value is 0.70 ± 0.04 below the pH_i prevailing before the application of NH_3/NH_4^+.

§This value is 0.47 ± 0.03 below the pH_i prevailing before the application of NH_3/NH_4^+.

dpH_i/dt in eight experiments on pattern-1 cells was 13 × 10^{-4} pH/s (pH_i = 6.71) with cells in 15.5 mM Na^+, and 40 × 10^{-4} pH/s when $[Na^+]_o$ was subsequently increased to 150 mM. The matched dpH_i/dt in these same pattern-1 cells under control conditions (first NH_4^+ pulse) averaged 42 ± 6.9 × 10^{-4} pH/s (mean pH_i = 6.83 ± 0.05; n = 8). Thus, regardless of which of the two 150-mM Na^+ values is used, reducing $[Na^+]_o$ to 15.5 mM caused the pH_i recovery rate to decrease by ~70% in these cells.

We made similar observations using two additional experimental protocols (protocols 2 and 3, summarized in Table III). Protocol 2 (Fig. 4 *B*) consisted of a single 85-s NH_3/NH_4^+ prepulse, followed by an exposure to solutions having $[Na^+]_o$ values of 15.5 and 150 mM (i.e., identical to the second half of Fig. 4 *A*). Again, in 16 osteoclasts we noted two patterns of pH_i recovery. In six pattern-2 cells, pH_i recovered rapidly, with an average dpH_i/dt of 23 ± 4.0 × 10^{-4} pH/s (mean

pH_i = 7.03 ± 0.07) in the presence of 15.5 mM Na^+. The mean rate of pH_i recovery in ten pattern-1 cells (those with slow recovery in 15.5 mM Na^+) increased from 6.3 × 10^{-4} pH/s (pH_i = 6.86) to 46 × 10^{-4} pH/s upon raising $[Na^+]_o$ from 15.5 to 150 mM (Table III). Protocol 3 (Fig. 4 *C*) was similar to protocol 2, except that the NH_3/NH_4^+ prepulse was followed by exposures to solutions having $[Na^+]_o$ values of 0, 15.5 and 150 mM. As in the previous two protocols, we noted two patterns of pH_i recovery. In the minority, pattern-2 cells, pH_i recovered rapidly ($dpH_i/dt > 18 \times 10^{-4}$ pH/s) in the absence of Na^+. In the pattern-1 cells, the pH_i recovery was virtually absent in Na^+-free solutions, as shown in Fig. 4 *C*. For these cells, dpH_i/dt ranged from -7×10^{-4} to $+4 \times 10^{-4}$ pH/s, having a mean value of -1.3×10^{-4}. When $[Na^+]_o$ was subsequently increased from 0 to 15.5 mM in the experiment shown in Fig. 4 *C*, pH_i recovered at a rate higher than observed for the other two protocols (i.e., when the cells had not been exposed to a Na^+-free solution). The mean maximal dpH_i/dt (measured at a mean pH_i of 6.66) for these pattern-1 cells in the presence of 15.5 mM Na^+ was 31 × 10^{-4} pH/s (Table III). Still in the 15.5 mM Na^+ solution, but just before $[Na^+]_o$ was increased to 150 mM, dpH_i/dt had decreased to 5.1 ± 1.3 × 10^{-4} pH/s (n = 21). Subsequently increasing $[Na^+]_o$ from 15.5 to 150 mM caused dpH_i/dt to increase to an average rate of 56 × 10^{-4} pH/s. Thus, at least in the pattern-1 cells, the recovery of pH_i from an acid load is markedly Na^+ dependent, consistent with the presence of a Na-H exchanger.

Recovery from Acid Loads Is Inhibited by Amiloride and 5-Amino-substituted Amiloride Analogues in Pattern-1 Cells

The Na-H exchangers of osteoclasts are active at resting pH_i. Most Na-H exchangers are characterized by their sensitivity to inhibition by amiloride and 5-amino-substituted amiloride derivatives (Kleyman and Cragoe, 1988). We therefore evaluated the effects of amiloride, ethylisopropylamiloride (EIPA) and hexamethyleneamiloride (HMA), employing three experimental protocols. The first is shown in Fig. 5 *A*. To test whether Na-H exchangers are active in the normal steady state, we examined the effect of applying 1 mM amiloride under resting conditions. This maneuver led to a reversible acidification that averaged 0.10 ± 0.01 pH units over a period of 116 ± 12 s (n = 7). The trajectory of the acidification was nearly linear, having a mean dpH_i/dt of −13 ± 2.0 × 10^{-4} pH/s, determined at an average pH_i = 7.24 ± 0.04. These results indicate that, under resting conditions, an amiloride-sensitive acid-extruder, presumably a Na-H exchanger, exactly balances background acid-loading processes.

The Na-H exchangers of osteoclasts are blocked by amiloride. Next, the cell shown in Fig. 5 *A* was acid loaded using a 85-s NH_3/NH_4^+ prepulse, and pH_i was allowed to recover under control conditions. At a mean pH_i of 6.91 ± 0.03, the maximal pH_i recovery rate averaged 37 ± 5 × 10^{-4} pH/s (n = 13) for this group of cells. After the pH_i recovery was complete, we applied a second 85-s NH_3/NH_4^+ prepulse, but this time introduced 1 mM amiloride during the NH_3/NH_4^+ washout. Again, we noted two patterns of pH_i recovery. In four pattern-2 cells, pH_i recovered rapidly, having an average dpH_i/dt of 30 ± 11 × 10^{-4} pH/s (mean pH_i = 6.76 ± 0.06) in the presence of amiloride. This was only modestly slower than the matched pH_i recovery in these same cells under control conditions after the first NH_4^+ pulse, 55 ± 6 × 10^{-4} pH/s (mean pH_i = 6.95 ± 0.02). In the remaining, pattern-1 cells (such as that illustrated

in Fig. 5 *A*), amiloride substantially reduced the rate of pH_i recovery, consistent with the presence of a Na-H exchanger. As summarized in Table IV (protocol 1), the maximal dpH_i/dt averaged 5.7×10^{-4} pH/s, considerably less than the matched pH_i recovery in these same cells under control conditions (first NH_4^+ pulse), 29×10^{-4} pH/s. Thus, 1 mM amiloride caused an 80% reduction in maximal recovery rates. In five cells (see Fig. 5 *A*), the inhibition was at least partially reversible, removal of amiloride causing dpH_i/dt to increase to an average maximum value of $18 \pm 5 \times 10^{-4}$ pH/s.

The pH_i recovery is Na^+ dependent and amiloride sensitive in the same cells (pattern-1). Our observation that osteoclasts display two patterns of pH_i recovery raises the question of whether the pH_i recovery is both Na^+ dependent and amiloride sensitive in the same cells. Therefore, we employed a second experimental protocol to answer this question. As shown in Fig. 5 *B*, cells were twice acid loaded by means of NH_3/NH_4^+ prepulses. During the first washout of NH_3/NH_4^+, $[Na^+]_o$ was reduced to 15.5 mM, whereas during the second washout, 1 mM amiloride was introduced in the presence of 150 mM Na^+. Consistent with our previous observations, we noted again two patterns of pH_i recovery. In three of 16 cells (i.e., pattern-2 cells), pH_i rapidly recovered from both acid loads, despite the lowered $[Na^+]_o$ or the presence of the amiloride (see discussion of Fig. 11 *B*, below). In the experiment on the pattern-1 cell illustrated in Fig. 5 *B*, however, recovery from the acute acid load was impeded at an $[Na^+]_o$ of 15.5 mM, but proceeded at higher rates once $[Na^+]_o$ was restored to 150 mM. Similarly, the pH_i recovery was greatly inhibited by amiloride after the second acid load. In 12 of 13 osteoclasts in which the pH_i recovery from the first acid load was substantially inhibited by 15.5 mM Na^+, amiloride profoundly reduced dpH_i/dt during the recovery from the second acid load. The mean dpH_i/dt for these 12 cells

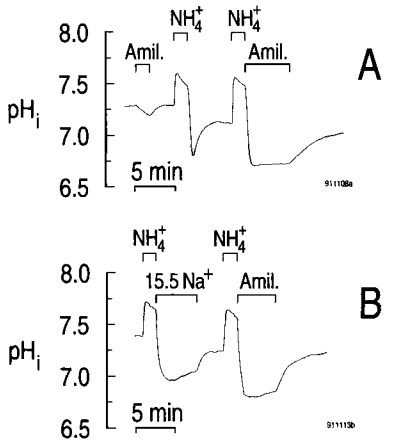

FIGURE 5. Recovery from acid loads in pattern-1 cells is amiloride sensitive. (*A*) A brief, 90-s application of 1 mM amiloride (*Amil.*), dissolved in solution 1, led to a reversible pH_i decrease of 0.11 under resting conditions. The osteoclast was subsequently acid loaded twice by means of 85-s NH_3/NH_4^+ prepulses (solution 2). In the first case, the cell recovered in solution 1. In the second, in which 1 mM amiloride was dissolved in solution 1, the pH_i recovery rate was inhibited >95%. Removal of the amiloride partially reversed this inhibition. (*B*) The osteoclast was twice acid loaded by means of 85-s NH_3/NH_4^+ prepulses (solution 2). After the first, reducing $[Na^+]_o$ to 15.5 mM (solution 4) caused pH_i to recover at a rate that was 87% reduced when compared to the rate of pH_i recovery observed when $[Na^+]_o$ was subsequently restored to 150 mM (solution 1). Recovery from the second acid load was largely blocked by 1 mM amiloride (dissolved in solution 1).

in the presence of amiloride after the second NH_4^+ pulse was 9.6×10^{-4} pH/s (see Table IV, protocol 2), not significantly different from the mean dpH_i/dt for these same cells in the presence of 15.5 mM Na^+ after the first NH_4^+ pulse, $8.8 \pm 1.1 \times 10^{-4}$ (mean $pH_i = 6.82 \pm 0.04$). However, both recovery rates are more than 70% lower than the matched control dpH_i/dt of 35×10^{-4} pH/s, observed when $[Na^+]_o$ was increased from 15.5 to 150 mM after the first NH_4^+ pulse.

High levels of EIPA and HMA cause a paradoxical alkalinization, and yet block Na-H exchange in osteoclasts. In a third protocol, we applied 50 μM EIPA or HMA while submitting the osteoclast to the solution changes shown in Fig. 6. Fig. 6 *A* shows a control experiment (same protocol as in Fig. 4 *C*), in which the osteoclast was acid loaded by prepulsing with NH_3/NH_4^+, and the subsequent pH_i recovery was monitored in the presence of 0, 15.5, and 150 mM Na^+. Fig. 6, *B* and *C*, show experiments otherwise identical to that in Fig. 6 *A*, except that we introduced either 50 μM EIPA

TABLE IV

*Effect of Amiloride on pH_i Recovery Rates**

Parameter	Protocol 1	Protocol 2
Control dpH_i/dt (10^{-4} pH/s) first NH_4^+ pulse	29 ± 6	35 ± 5
pH_i at control dpH_i/dt	6.89 ± 0.04	6.95 ± 0.05
Amiloride dpH_i/dt (10^{-4} pH/s) second NH_4^+ pulse	5.7 ± 1.3	9.6 ± 1.2
pH_i at amiloride dpH_i/dt	6.69 ± 0.05	6.81 ± 0.03
Inhibition	80%	73%
P value‡	0.007	0.0003
n	9	12

*In protocol 1 (Fig. 5 *A*), the osteoclast was twice acid loaded via NH_3/NH_4^+ prepulses. After the first acid load, the NH_3/NH_4^+ was washed out into a solution containing 150 mM Na^+ (control dpH_i/dt). After the second, the NH_3/NH_4^+ was washed out into a solution containing 150 mM Na^+ plus 1 mM amiloride (amiloride dpH_i/dt). Also recorded are the pH_i values at which the two dpH_i/dt values were measured. In protocol 2 (Fig. 5 *B*), the osteoclast also was twice acid loaded via NH_3/NH_4^+ prepulses. After the first, the NH_3/NH_4^+ was washed out into a solution containing 15.5 mM Na^+. This was then switched to one containing 150 mM Na^+ (control dpH_i/dt). After the second acid load, the NH_3/NH_4^+ was washed out into a solution containing 150 mM Na^+ plus 1 mM amiloride (amiloride dpH_i/dt).

‡The *P* value is the result of a paired *t* test comparing control and amiloride dpH_i/dt values.

or HMA while the extracellular solution still was Na^+ free. We were surprised to find that EIPA, but particularly HMA, alkalinized the cell even in the absence of Na^+ (arrow at *A* in Figs. 6, *B* and *C*). For EIPA, the mean rate of alkalinization was $+10 \pm 2.3 \times 10^{-4}$ pH/s ($n = 4$), and for HMA, $+22 \pm 1.8 \times 10^{-4}$ pH/s ($n = 5$). The application of 0.1% (vol/vol) DMSO, the vehicle in which both EIPA and HMA were dissolved, did not significantly affect the rate of pH_i change ($n = 5$). In general, the EIPA- or HMA-induced alkalinizations were self limited and reversible, as shown for HMA in Fig. 6 *C*. Even though these compounds, employed at concentrations of 50 μM, paradoxically increased pH_i, they nevertheless inhibited Na-H exchange. Thus, we observed no appreciable increase in the dpH_i/dt upon raising $[Na^+]_o$ from 0 to 15.5 mM (*arrow* at *b* in Fig. 6, *B* and *C*) or from 15.5 to 150 mM (*arrow c*). The mean data for these experiments are summarized in Table V. We did not examine the effects of EIPA or HMA on pH_i in the pattern-2 cells.

We however observed that the pH_i increase elicited by applying EIPA or HMA was associated with a substantial decrease in the I_{440} signal (segment *ad*, Fig. 6 *D*), whereas the pH_i decrease elicited by withdrawing EIPA or HMA was associated with an increase in the I_{440} signal (segment *de*, Fig. 6 *D*). To investigate the possibility that these effects were caused by an unknown interaction of the amiloride analogues with

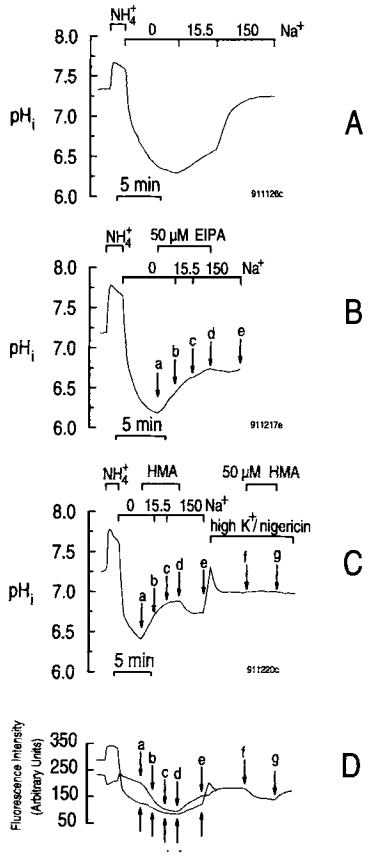

FIGURE 6. Na-H exchange in pattern-1 rat osteoclasts is highly sensitive to inhibition by 5-amino-substituted amiloride analogues. (*A*) Control experiment showing the Na^+ dependence of the pH_i recovery from an acid load. After acid loading via an NH_3/NH_4^+ prepulse (solution 2), pH_i did not recover in the nominal absence of external Na^+ (solution 5). Raising $[Na^+]_o$ from 0 mM to 15.5 mM (solution 4) caused pH_i to recover at a rate that was 87% of the rate observed after restoring $[Na^+]_o$ to 150 mM (solution 1). (*B*) Na-H exchange is blocked by ethylisopropylamiloride (EIPA). Applying 50 μM EIPA in the absence of Na^+ causes pH_i to increase (*arrow a*). The trajectory of the pH_i increase was not accelerated by raising $[Na^+]_o$ to either 15.5 mM (solution 4, *arrow b*) or 150 mM (solution 1, *arrow c*). After removal of EIPA (*arrow d*), pH_i decreased and then started to increase slowly (*segment de*). (*C*) Na-H exchange is blocked by hexamethyleneamiloride (HMA). The first part of the protocol is identical to that of *B*, except that the cell was exposed to 50 μM HMA, rather than EIPA. Removal of HMA (*arrow d*), led to a marked cytoplasmic acidification (*segment de*). All experiments were concluded by exposing the cell to a high-K^+/10-μM nigericin solution (solution 3) at pH 7.00, thereby clamping pH_i to this value. In this experiment, a second pulse of 50 μM HMA (*segment fg*) was applied in the presence of the high-K^+/nigericin. Under these conditions, HMA failed to increase pH_i. (*D*) Time courses of the I_{440} (*labeled arrows*) and I_{490} (*unlabeled arrows*) signals from the same experiment shown in *C*. The first application of HMA caused a substantial fall in I_{440}, but less so in I_{490} (*segment ad*). Upon removal of the drug (*arrow d*), both I_{440} and I_{490} recovered (*segment de*). Exposing the osteoclast to high-K^+/10-μM nigericin equalized I_{440} and I_{490}. Applying 50 μM HMA under these conditions (*arrow f*) caused reversible but identical decreases in both I_{440} and I_{490} (*segment fg*).

BCECF, or by interference with the measurement of BCECF fluorescence, we applied HMA while clamping pH_i to 7.00 by exposing the cell to a high-K^+/nigericin solution. As illustrated by the last portion of Fig. 6 *C*, 50 μM HMA failed to change pH_i. Under these conditions, HMA caused both the I_{440} and I_{490} signals to decrease

slightly and to the same extent (segment *fg*, Fig. 6 *D*). Similar results were obtained in two other experiments.

Removal of the amiloride analogues, in the continued presence of 150 mM Na^+, caused either a transient slowing of the pH_i increase (not shown), a modest acidification (segment *de* for EIPA in Fig. 6 *B*) or a pronounced acidification (*de* for HMA in Fig. 6 *C*). In the case of EIPA withdrawal, dpH_i/dt temporarily slowed to an average of $1.5 \pm 2.6 \times 10^{-4}$ pH/s, but increased again within 3 min to $7–14 \times 10^{-4}$ pH/s. In the case of HMA withdrawal, the cytoplasm acidified within 3 min an average of 0.12 ± 0.01 pH units, after which the cells started to recover slowly ($<6 \times 10^{-4}$ pH/s).

Virtually identical results were obtained in experiments after a protocol similar to that shown in Fig. 4 *A*, except that 50 μM EIPA ($n = 12$) or 50 μM HMA ($n = 8$) were added to the 15.5 mM and 150 mM Na^+-containing solutions that were applied to

TABLE V

*Effect of High Concentrations of Amiloride Analogues on pH_i Recovery Rates**

$[Na^+]_o$	Drug status	Experiments in which 50 μM EIPA was applied		Experiments in which 50 μM HMA was applied	
		dpH_i/dt	pH_i at dpH_i/dt	dpH_i/dt	pH_i at dpH_i/dt
mM		*10^{-4} pH/s*		*10^{-4} pH/s*	
0	Absent	-8.3 ± 3.0	6.35 ± 0.04	-5.8 ± 2.6	6.57 ± 0.05
0	Present	10 ± 2.3‡	6.35 ± 0.04	22 ± 2‡	6.57 ± 0.05
15.5	Present	11 ± 1.4^{NS}	6.46 ± 0.04	16 ± 3^{NS}	6.79 ± 0.07
150	Present	8.8 ± 2.3^{NS}	6.57 ± 0.04	-2.2 ± 5.0§	6.91 ± 0.07
150	Removed	1.5 ± 2.6§	6.64 ± 0.04	-14 ± 2^{NS}	6.91 ± 0.08
n		4		5	

*The protocols for these experiments were those for Fig. 6 *B* (EIPA added) and Fig. 6 *C* (HMA added). The first row ($[Na^+]_o = 0$, drug absent) represents data taken just before point *a* in the figures. The second row represents data taken just after point *b*, and so on. The fifth row represents data taken just before *e*.

^{NS}The value is not significantly different from the one immediately above it (paired *t* test).

‡The value is significantly greater than the one immediately above it ($P = 0.002$).

§The value is significantly less than the one immediately above it ($P = 0.03$ for the EIPA column, $P = 0.01$ for the HMA column).

the cell after the second NH_3/NH_4^+ prepulse. In all 20 experiments, the amiloride analogues prevented the pH_i recovery upon raising $[Na^+]_o$ from 15.5 to 150 mM, further establishing that acid extrusion in pattern-1 cells is mediated by Na-H exchange.

Intrinsic Buffering Power in Pattern-1 Cells

To convert rates of pH_i change to acid-base fluxes, we determined the pH_i dependence of intrinsic intracellular buffering power, β_I. Our approach was to expose acid-loaded osteoclasts to a Na^+-free solution containing 20 mM NH_3/NH_4^+, and then decrease $[NH_3/NH_4^+]_o$ to 0 mM in a step-wise fashion. This caused pH_i to also decrease in a step-wise fashion, as shown in Fig. 7 *A*. For each step, we computed β_I from the ΔpH_i and the computed $\Delta[NH_4^+]_i$, as described in Methods. To exclude

interference from background acid-loading or -extruding processes, we discarded steps for which the initial or final pH_i baseline drifted more rapidly than $\pm 5 \times 10^{-4}$ pH/s. Fig. 7 *A* shows one of three experiments in which the absolute value of dpH_i/dt at all seven pH_i values was 5×10^{-4} pH/s or less, indicating the absence of substantial acid-loading or -extruding processes. Fig. 7 *B* summarizes the results averaged from a total of 19 osteoclasts, and shows that β_I falls with increasing pH_i values, from a high of 25 mM/pH at a pH_i of 6.41 to a low of 6.2 mM/pH at a pH_i of 7.36. The solid curve drawn through the points is the result of a fit to a second-order polynomial.

The broken curve represents the results of a fit to the equation describing the buffering power of a single monoprotic weak acid, as described by Wilding, Cheng,

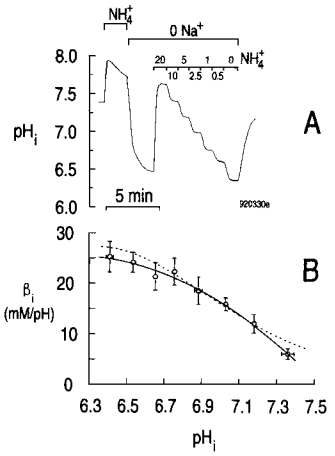

FIGURE 7. The intrinsic buffering power (β_I) of rat osteoclasts falls with increasing pH_i. (*A*) pH_i record from a pattern-1 osteoclast. The cell was acid loaded by means of an NH_3/NH_4^+ prepulse (solution 2), and then exposed to a nominally Na^+-free saline (solution 5) during application and subsequent step-wise reduction of extracellular NH_3/NH_4^+. The solutions containing the indicated concentrations of NH_4^+ were prepared by mixing solutions 5 and 6. Restoration of $[Na^+]_o$ to 150 mM caused pH_i to increase, indicating the activity of Na-H exchange. From these data, β_I is calculated as described in Materials and Methods. (*B*) Summary of the data obtained from 19 osteoclasts submitted to the solution changes shown in *A*. The average dpH_i/dt value observed at the time pH_i measurements were made was $-1.5 \pm 0.25 \times 10^{-4}$ pH/s ($n = 82$). The 64 (pH_i, β_I) pairs calculated from these pH_i data were divided into eight sets of eight and averaged for β_I and pH_i. Vertical and horizontal bars indicate SEM, and are omitted if the SEM is not at least 25% greater than the size of the symbol. A second-order polynomial function, $\beta_I = -523 + 177 \times pH_i - 14.3 \times (pH_i)^2$, was fitted to the data (*solid curve*). The theoretical β vs pH relationship of a weak monoprotic acid with a total concentration 47 ± 3.9 (SD) mM and an apparent pK_a of 6.34 ± 0.09 (SD) was also fitted to the data (*broken curve*).

and Roos (1992). The best-fit values are a total buffer concentration of 47 ± 4 (SD) mM and an apparent pK_a of 6.34 ± 0.09 (SD).

Osteoclast Na-H Exchangers Are Highly Sensitive to HMA in Pattern-1 Cells

So far, we showed that, in the nominal absence of CO_2/HCO_3^-, the majority of osteoclasts recover from acute acid loads in a pH_i dependent fashion, and that the recovery rates are reduced by lowering $[Na^+]_o$ or by applying amiloride or its derivatives. These data are consistent with the presence of Na-H exchangers in the plasma membrane of rat osteoclasts. Based on the sensitivity of Na-H exchangers to amiloride analogues, these transporters can be grouped into three categories: (*a*)

Na^+-dependent, CO_2/HCO_3^--independent acid-extruders that appear to be Na-H exchangers, but are insensitive to amiloride analogues. These have been reported in cultured rat hippocampal neurons (Raley-Susman, Cragoe, Sapolsky, and Kopito, 1991) and freshly isolated rat hippocampal pyramidal neurons (Schwiening and Boron, 1994). (*b*) Na-H exchangers that are mildly sensitive to amiloride analogues. These are typified by exchangers found at the apical membranes of epithelia (Clark and Limbird 1991). (*c*) Na-H exchangers that are highly sensitive to amiloride and its derivatives. By the definition of Clark and Limbird (1991), these exchangers have a 50% inhibitory concentration (IC_{50}) for 5-amino-substituted amiloride analogues that is < 1 μM in the presence of physiological amounts of Na^+. These exchangers are found in many nonepithelial cells and at the basolateral membrane of epithelia, and at least some are encoded by NHE1 cDNA.

To classify the Na-H exchangers of rat osteoclasts, we determined the IC_{50} for HMA by monitoring pH_i recovery rates from acute acid loads after raising $[Na^+]_o$ from 0 to 150 mM in the presence of 0–10 μM HMA. To permit determination of dpH_i/dt over a wide range of pH_i values, we increased the duration of the NH_3/NH_4^+ prepulse, such that washout of the NH_3/NH_4^+ into a Na^+-free solution drove pH_i to values between 6.25 and 6.50. In the absence of HMA, subsequently raising $[Na^+]_o$ from 0 to 150 mM caused the pH_i recovery, at a pH_i of 6.85, to proceed at a rate of $134 \pm 24 \times 10^{-4}$ pH/s ($n = 12$). This value is substantially higher than the comparable dpH_i/dt of $36 \pm 3.9 \times 10^{-4}$ pH/s ($n = 15$; $P = 0.002$) observed when the NH_3/NH_4^+ was washed out directly into our standard HEPES solution containing 150 mM Na^+. This higher dpH_i/dt when the NH_3/NH_4^+ was washed out into a Na^+-free solution probably reflects the relatively low $[Na^+]_i$, as reported in other cells (Grinstein, Cohen, and Rothstein, 1984; Green, Yamaguchi, Kleeman, and Muallem, 1988; Paradiso, 1992). As is shown in Fig. 8 *A*, HMA caused a dose-dependent decrease in pH_i recovery rate. Note that neither the application of 10 μM HMA (Fig. 8 *A*) nor the withdrawal of 10 μM HMA (not shown) produced a discernible alkalinization or acidification, respectively. Thus, the paradoxical alkalinization elicited by HMA (see Fig. 6 *C*) occurs only at doses > 10 μM.

Fig. 8 *B* summarizes the effect of HMA on total net acid-extrusion rate (J_{total}). The latter was computed as the product of dpH_i/dt (determined at pH_i 6.60) and β_I (computed at pH_i 6.60 from the regression coefficients of the polynomial describing the pH_i dependence of β_I in Fig. 7 *B*). Using a nonlinear least-squares approach, and assuming a single population of Na-H exchangers, we fitted the Michaelis-Menten equation to the fractional-inhibition-vs-$[HMA]_o$ data obtained from 47 osteoclasts. For data obtained at a pH_i of 6.60, the K_I was 49 ± 13 nM (mean ± SD; Fig. 8 *B*, *inset*). Similar results were obtained when the fluxes were determined at pH_i values of 6.5, 6.7, 6.8, or 6.9.

$[Na^+]_o$ Dependency of the Na-H Exchange in Pattern-1 Cells

To estimate the dependence of Na-H exchange on $[Na^+]_o$, we determined rates of pH_i recovery from acid loads at a pH_i of 6.60 in the presence of increasing $[Na^+]_o$. We employed a protocol similar to that of Fig. 4 *C*, in which we prepulsed with NH_3/NH_4^+ for at least 85 s, washed the NH_3/NH_4^+ out into a Na^+-free solution, allowed pH_i to stabilize, and then exposed the cell to a solution containing either 7.5, 15, 30,

45, 60, 100, or 150 mM Na^+. Finally, in each case except the last, we switched to a solution containing 150 mM Na^+. Osteoclasts exhibiting a pH_i recovery in the nominal absence of Na^+ (pattern-2 cells) were excluded from this analysis. Fig. 9 *A* shows representative pH_i records. As expected for Na-H exchange, the pH_i recovery rate was greater with increasing $[Na^+]_o$. Fig. 9 *B* summarizes the $[Na^+]_o$ dependence of J_{total} at a pH_i of 6.60 for 88 osteoclasts. Using a nonlinear least-squares curve fitting procedure to fit the Hill equation to these data yielded a K_m of 45 ± 5.0 (SD) mM, an apparent Hill coefficient (n_H) of 1.2 ± 0.2 (SD), and a maximal flux 628 ± 165 (SD) μM/s. The best-fit n_H is consistent with a Hill coefficient of unity.

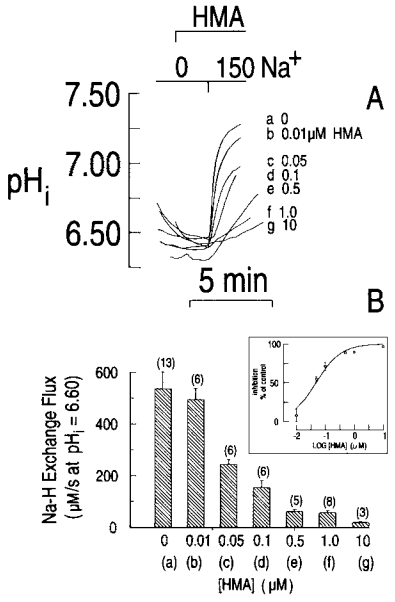

FIGURE 8. The Na-H exchanger of rat osteoclasts is highly sensitive to inhibition by HMA. (*A*) Switching the cells from 0 (solution 5) to 150 mM Na^+ (solution 1) in the presence of hexamethyleneamiloride (HMA) leads to a dose-dependent decrease in the rate of acid-load recovery. The cytoplasmic acid load was delivered by means of a NH_3/NH_4^+ prepulse (solution 2) that is not shown. Superimposed pH_i transients of eight different osteoclasts at increasing concentrations HMA are shown. The concentration HMA in μM is given after the letters (*a,b,. . ., g*). The pH_i transient labeled *a* was recorded in the presence of 0.1% (vol/vol) DMSO. Note that the application of HMA does not induce the alkalinization seen with 50 μM of the drug at any of the concentrations used. (*B*) Summary of the data obtained from 47 osteoclasts submitted to the solution changes shown in *A*. The number of observations used to determine the average Na-H exchange flux at pH_i = 6.60 is shown in parentheses above the vertical bars. (*Inset*) Fitting the Michaelis-Menten equation to the % inhibition-vs-$[HMA]_o$ data, yielded an K_I of 49 ± 13 (SD) nM. Vertical bars represent the SEM, and are omitted if the SEM is not at least 25% greater than the radius of the symbol.

pH_i Dependency of Na-H Exchange in Pattern-1 Cells

During the recovery of pH_i from an acute acid load, J_{total} is the result of fluxes due to Na-H exchange ($J_{Na\text{-}H}$) as well as to fluxes due to other acid-loading or extrusion processes resistant to amiloride ($J_{amil/R}$). Thus, if we assume that the only action of amiloride is to block Na-H exchange by 100%, $J_{Na\text{-}H}$ is the difference between J_{total} and $J_{amil/R}$. We determined $J_{amil/R}$ values in two ways. First, we determined rates of pH_i decrease produced by the application of 1 mM amiloride under resting conditions (see first application of amiloride in Fig. 5 *A*), and multiplied the dpH_i/dt values, obtained at pH_i intervals of 0.05, by the corresponding β_I. The latter were obtained from the regression coefficients of the second-order polynomial describing the pH_i

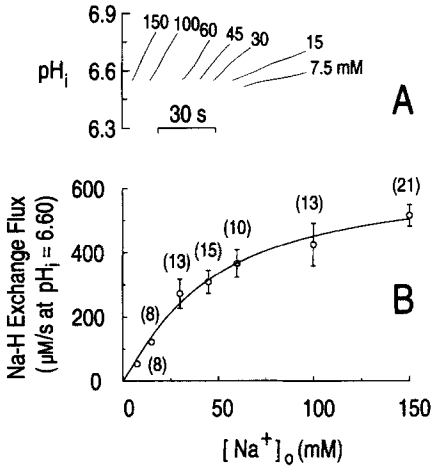

FIGURE 9. $[Na^+]_o$ dependency of Na-H exchange in pattern-1 cells. (*A*) Osteoclasts were acid loaded by means of a NH_3/NH_4^+ prepulse (solution 2) and switched to a nominally Na^+-free solution (solution 5). Next, pH_i was allowed to reach a stable value (not shown) before the cell was exposed to a solution containing the indicated Na^+ concentration in millimolar. Solutions containing < 150 mM Na^+ were prepared by mixing solution 5 and a solution identical to solution 1 except that it contained exactly 120 mM NaCl in addition to ~30 mM NMDG-Cl. The final Na^+ concentration of all solutions used was confirmed with a flame photometer. Representative parts of the pH_i traces are shown. (*B*) Summary of the data obtained from 88 osteoclasts submitted to the solution changes described in *A*. The number of cells used to determine the average Na-H exchange flux at pH_i = 6.60 as a function Na_o^+ is shown in parentheses. To these data, the Hill equation was fitted. The best fit required a K_m of 45 ± 5.0 (SD) mM, an apparent Hill coefficient (n_H) of 1.2 ± 0.2 (SD), and a maximal flux 628 ± 165 (SD) μM/s.

dependence of β_I (Fig. 7 *B*). The resultant amiloride-resistant acid-loading fluxes are represented by the negative values in Fig. 10 *A* (*inset*). Second, we determined rates of pH_i increase, after an acid load imposed by an NH_3/NH_4^+ prepulse, while exposing the cell to 1 mM amiloride (see second application of amiloride in Fig. 5 *A*). These data yielded fluxes due to amiloride-resistant acid-extruding mechanisms, and are represented by the positive values in the inset of Fig. 10 *A*. In the pH_i range

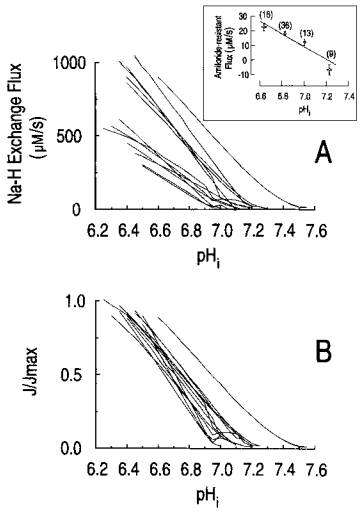

FIGURE 10. pH_i dependency of Na-H exchange in pattern-1 cells. (*A*) Na-H exchange fluxes, corrected for the amiloride-resistant flux, as a function of pH_i observed in 13 osteoclasts. (*Inset*) The amiloride-resistant flux vs pH_i relationship. To these data, a straight line with a slope of 43 ± 6 (SD) μM/(s.pH) and an intercept of 310 ± 40 (SD) μM/s was fitted. (*B*) Na-H exchange fluxes shown in *A* normalized for their individual maximal predicted Na-H exchange flux (J/J_{max}) as a function of pH_i.

6.5–7.3, the $J_{amil/R}$ values (obtained from a total of 21 cells) increased approximately linearly from +30 (acid extrusion) to −10 (acid loading) μM/s.

We obtained the pH_i dependence of J_{total} in 13 experiments performed according to the protocol shown in Fig. 8 *A* (record *a*). The dpH_i/dt values at pH_i 6.6 for these cells are summarized in column *a* of Fig. 8 *B*. For each of the 13 experiments, we computed J_{total} at pH_i intervals of 0.05 by multiplying the dpH_i/dt values by the corresponding β_I values. Subtracting the best-fit values for $J_{amil/R}$ (Fig. 10 *A*, *inset*) from J_{total} yielded the 13 $J_{Na\text{-}H}$ vs pH_i relationships shown in Fig. 10 *A*. The magnitude of $J_{Na\text{-}H}$ values varied widely from cell to cell, from as little as 250 μM/s at a pH_i of 6.5, to as much as 1,000 μM/s. Regardless of its magnitude, $J_{Na\text{-}H}$ decreased markedly with increasing pH_i.

Because intracellular protons appear to cooperatively activate Na-H exchange in other cells (Aronson, 1985), we fitted the Hill-equation to our data to estimate the apparent Hill coefficient (n_H), as well as the maximal $J_{Na\text{-}H}$. For each of the 13 experiments, we used a nonlinear least-squares curve fitting procedure to estimate J_{max}, and then normalized the $J_{Na\text{-}H}$ data for that experiment by its J_{max}. Fig. 10 *B* shows the normalized $J_{Na\text{-}H}$ vs pH_i plots for each of the experiments. The mean J_{max} was 741 ± 82 μM/s, whereas the mean n_H was 2.9 ± 0.1. Finally, $J_{Na\text{-}H}$ was half maximal at a mean pH_i of 6.73 ± 0.02.

Evidence for the Presence of Proton Pumps in Pattern-2 Cells

Incidence, morphology and initial pH_i of pattern-2 cells. As noted above, we found that, in a minority (~20% overall) of osteoclasts plated on glass, pH_i recovered rapidly from acid loads even if we reduced $[Na^+]_o$ to 15.5 or 0 mM, or if we introduced amiloride. Among cells for which we examined the pH_i recovery from acid loads at an $[Na^+]_o$ of 15.5 mM, 11 out of 29 (38%) had high dpH_i/dt values, as defined above, and thus are classified as pattern-2 cells. Similarly, 29 of 224 (13%) cells in which the recovery was examined in the absence of Na^+ fulfilled the pattern-2 criterion, as did 7 of 29 (24%) cells examined in the presence of amiloride. Interestingly, 55% (6/11) of the cells classified as pattern-2 by the 15.5-mM Na^+ protocol were round, as were 86% (25/29) of the osteoclasts classified by the 0-Na^+ protocol and 57% (4/7) classified by the amiloride protocol. Even though 74% (35/47) of the pattern-2 cells were round, only slightly less than half (22/53 or 42% by the 0-Na^+ protocol) of the round osteoclasts were pattern-2 cells.

For the 47 pattern-2 cells identified on the basis of either the 15.5-mM Na^+ protocol, the 0-Na^+ protocol, or the amiloride protocol, the mean initial pH_i was 7.47 ± 0.03. This is 0.16 higher than the average initial pH_i values of the entire osteoclast population, which includes the 47 pattern-2 cells.

Recovery of pH_i from acid loads in pattern-2 cells in the absence of Na^+. 29 pattern-2 cells were identified by their recovery from an acid load in the absence of Na^+. An example is shown in Fig. 11 *A*. In these osteoclasts, the maximal recovery rates averaged 38 ± 5 × 10^{-4} pH/s, as determined at an average pH_i = 7.09 ± 0.05. This dpH_i/dt value is substantially higher than the value of −1.3 × 10^{-4} pH/s observed in pattern-1 cells under similar 0-Na^+ conditions (see Table III, protocol 3). In 16 of the 29 experiments, we permitted the cell to recover from the acid load until pH_i

stabilized. The average final pH_i for these 16 osteoclasts was 7.27 ± 0.05, which was 0.25 lower than the initial pH_i (7.52 ± 0.05) for these cells ($P = 3 \times 10^{-5}$).

Effect of Na^+ readdition in pattern-2 cells. In 9 of the 16 cells for which we allowed pH_i to stabilize in the absence of Na^+ (see above), increasing $[Na^+]_o$ from 0 to 150 mM had no discernible effect on pH_i. An example is the first NH_4^+ pulse in Fig. 11 *A* (*arrow*). The mean final pH_i for these nine cells in which Na^+ failed to elicit a further pH_i recovery was 7.33 ± 0.06, which was 0.20 ± 0.05 lower than the initial pH_i for

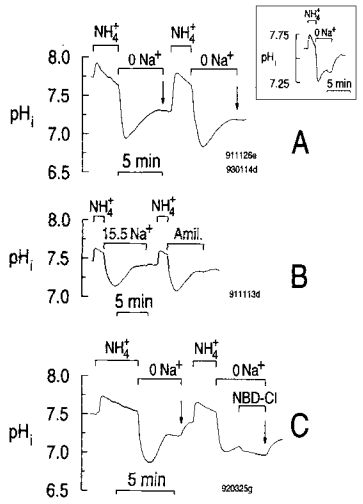

FIGURE 11. In pattern-2 cells, pH_i recovery from acid loads is independent of Na^+, insensitive to amiloride, but blocked by NBD-Cl. (*A*) Recovery of pH_i from acid loads in a pattern-2 cell exposed to a nominally Na^+-free solution. The osteoclast was twice acid loaded by means of a NH_3/NH_4^+ prepulse (solution 2), and exposed to a 0-Na^+ saline (solution 5). Despite the absence of Na^+, pH_i recovered briskly both times. Restoring the extracellular Na^+ did not elicit any further pH_i increase (*arrow*). (*Inset*) Example of a pattern-2 cell in which restoring extracellular Na^+ to 150 mM (solution 1) led to a further pH_i increase. (*B*) Recovery of pH_i from acid loads in a pattern-2 cell exposed to either a low-Na^+ solution, or a 150-mM Na^+ solution containing 1 mM amiloride. The osteoclast was twice acid loaded by means of a NH_3/NH_4^+ prepulse (solution 2). The pH_i recovery from the first acid load proceeded rapidly, even though $[Na^+]_o$ was only 15.5 mM (solution 4), and the recovery from the second acid load was brisk despite the presence of 1 mM amiloride (dissolved in solution 1). The solutions and the preparation of osteoclasts were the same as used in the experiment shown in Fig. 5 *B* (a pattern-1 cell). Note that neither increasing $[Na^+]_o$ to 150 mM (first pulse) nor removing the amiloride (second pulse) led to a further pH_i recovery. (*C*) Blockade of the pH_i recovery from an acid load in a pattern-2 cell exposed to 7-chloro-4-nitrobenz-2-oxa-1,3-diazol (NBD-Cl), a known vacuolar-type proton pump blocker. The osteoclast was twice acid loaded by means of a NH_3/NH_4^+ prepulse (solution 2). Despite the nominal absence of external Na^+ (solution 5), pH_i recovered from the first acid load; raising $[Na^+]_o$ to 150 mM caused pH_i to increase further (*arrow*). After the second acid load, the pH_i recovery in the nominal absence of Na^+ was interrupted by applying 100 μM NBD-Cl to the cell (dissolved in solution 5), which unmasked an acid-loading process. Restoring $[Na^+]_o$ to 150 mM caused a further alkalinization (*arrow*).

these cells ($P = 0.005$). That Na^+ failed to increase pH_i in these cells implies that Na-H exchangers were inactive, at least at such an alkaline pH_i. In the remaining seven osteoclasts, pH_i after recovery from the acid load in the 0-Na^+ solution stabilized at a lower value, 7.20 ± 0.09. In these cells, increasing $[Na^+]_o$ from 0 to 150 mM resulted in a further pH_i recovery, consistent with Na-H exchange activity. An example is given in the inset of Fig. 11 *A*. The initial rate of these Na^+-induced pH_i recoveries averaged 71 ± 33 $\times 10^{-4}$ pH/s; the total increase in pH_i averaged

0.23 ± 0.08. It is noteworthy that this Na-H exchange activity occurred over a much higher pH_i range than seen in a typical pattern-1 cell (see Fig. 10). After the Na^+-induced alkalinization, pH_i in these seven cells averaged 7.43 ± 0.12. In a paired *t* test, the final pH_i after Na^+ readdition for these seven cells was not significantly different from the initial pH_i, 7.52 ± 0.07 ($P = 0.24$).

In eight of the experiments on pattern-2 cells, in which we allowed pH_i to stabilize in the absence of Na^+ and then increased $[Na^+]_o$ to 150 mM, we acid loaded the osteoclast a second time. An example of such an experiment is shown in Fig. 11 *A*. The results are summarized in Table VI. We found that, for the second pH_i recovery, neither the maximal rate of pH_i recovery nor the final value to which pH_i recovered was significantly different from the corresponding value for the first pH_i recovery.

Na^+ independence and amiloride insensitivity of the pH_i recovery in the same pattern-2 cells. When we initially distinguished between pattern-1 and -2 cells, we identified 11 pattern-2 cells (five according to protocol 1, and six according to protocol 2 of Table III) solely on the basis of a relatively rapid dpH_i/dt in the presence of 15.5 mM Na^+. We identified an additional four pattern-2 cells (according to the protocol of Table IV) solely on the basis of a relatively rapid pH_i recovery in the presence of 1 mM amiloride and 150 mM Na^+. To determine whether the pH_i recovery is both Na^+ independent and amiloride insensitive in the same cells, we subjected cells to the protocol shown in Fig. 11 *B*. We first examined the recovery of pH_i from an acid load in the presence of 15.5 mM Na^+, after which we increased $[Na^+]_o$ to 150 mM. Next, we acid loaded the osteoclast a second time, and examined the pH_i recovery in the presence of 1 mM amiloride. As is shown in the figure, the same osteoclast that had a rapid pH_i recovery at reduced $[Na^+]_o$ also had a rapid recovery in the presence of amiloride. In three cells, the average maximal pH_i recovery rate was 28 ± 8.3 × 10^{-4} pH/s (pH_i = 7.08 ± 0.14) at low $[Na^+]_o$, and 24 ± 2.6 × 10^{-4} pH/s (pH_i = 7.03 ± 0.12) in the presence of amiloride.

Sensitivity of the pH_i recovery to NBD-Cl in pattern-2 cells studied in the absence of Na^+. These above data indicate that a subgroup of osteoclasts express a robust,

TABLE VI

*Comparison of pH_i Recoveries after Paired NH_3/NH_4^+ Pulses under 0-Na^+ Conditions in Pattern-2 Cells**

Parameter	First pulse	Second pulse	*n*	Significance
Minimum pH_i	7.08 ± 0.07	6.88 ± 0.05	8	0.001
Initial vs minimum pH_i	−0.54 ± 0.03	−0.55 ± 0.07	8	NS
Max dpH_i/dt (10^{-4} pH/s)	33 ± 7	37 ± 5	8	NS
pH_i at Max dpH_i/dt	7.12 ± 0.08	6.96 ± 0.07	8	0.003
Final pH_i	7.33 ± 0.07	7.27 ± 0.07	8	NS

*The experiments followed the protocol of Fig. 11 *A*. Minimum pH_i is the lowest pH_i achieved after washout of NH_3/NH_4^+. Max dpH_i/dt is the maximal rate of pH_i recovery, measured at pH_i at max dpH_i/dt; this pH_i is slightly higher than the minimum pH_i. dpH_i/dt at pH_i 6.9 is the pH_i recovery rate measured at a pH_i of 6.9. Initial vs minimum pH_i is the difference between the pH_i value prevailing before application of the NH_3/NH_4^+ and the minimum pH_i. Final pH_i is the value prevailing after recovery of pH_i from the acid load in the absence of Na^+ was complete, or nearly so. *n* is the number of observations. Significance was judged on the basis of paired *t* tests, comparing values for the first and second pulses.

Na^+-independent, amiloride-insensitive acid-extrusion mechanism. To test the hypothesis that the pH_i recovery from acid loads under nominally Na^+-free conditions is brought about by a plasma membrane H^+ pump, we examined the effect of 7-chloro-4-nitrobenz-2-oxa-1,3-diazol (NBD-Cl), a potent inhibitor of vacuolar-type proton pumps (Forgac, 1989). In the experiment shown in Fig. 11 *C*, we twice monitored the recovery of pH_i from acid loads. The recovery from the first acid load occurred in the absence of Na^+, indicating the presence of a potent, Na^+-independent acid-extrusion mechanism. After the readdition of Na^+, which led to a further pH_i recovery (*first arrow* in Fig. 11 *C*), the osteoclast was acid loaded a second time. However, we interrupted the pH_i recovery from this second acid load with 100 μM NBD-Cl, which not only blocked the further pH_i recovery, but unmasked a slow background acidification. In three such experiments, as well as eight similar ones in which the first NH_4^+ pulse was omitted, NBD-Cl greatly decreased the rate of pH_i recovery. The drug was applied after the pH_i recovery had proceeded from an average pH_i of 7.00 ± 0.12 to 7.14 ± 0.11. At the latter pH_i value (i.e., before the addition of NBD-Cl), dpH_i/dt was 30 ± 7 × 10^{-4} pH/s (n = 11). In three of the 11 cells, addition of NBD-Cl caused dpH_i/dt to approach zero; for these cells, the mean dpH_i/dt in the presence of NBD-Cl was +3.7 ± 1.9 × 10^{-4} pH/s (n = 3). The paired dpH_i/dt before the addition of NBD-Cl was +7.7 ± 1.7 × 10^{-4} pH/s (n = 3). In the other eight cells, NBD-Cl actually caused pH_i to decline (as in Fig. 11 *C*). For these cells, the mean dpH_i/dt in the presence of NBD-Cl was −74 ± 31 × 10^{-4} pH/s (n = 8); dpH_i/dt averaged 39 ± 8 × 10^{-4} pH/s (n = 8) before the application of the blocker. This NBD-Cl-induced acidification is consistent with the unmasking of an acid-loading process, possibly Na-H exchange operating in reverse in the absence of external Na^+. In addition, it suggests that the rate of pH_i recovery observed in the absence of NBD-Cl underestimates the contribution of the H^+ pump. From the mean dpH_i/dt in the absence of NBD-Cl (30 × 10^{-4} pH/s; n = 11), and the mean dpH_i/dt in the presence of the drug (−53 × 10^{-4} pH/s; n = 11), we calculate that the rate of pH_i recovery due to the H^+ pump is 83 × 10^{-4} pH/s at a mean pH_i value of 7.14.

In the pH_i recovery from the second NH_4^+ pulse in Fig. 11 *C*, simultaneously restoring $[Na^+]_o$ to 150 mM and removing the NBD-Cl caused pH_i to recover rapidly. We made similar observations in seven other experiments in which the Na^+ was returned in the continuous presence of NBD-Cl. The mean Na^+-dependent dpH_i/dt in these seven experiments was 65 ± 28 × 10^{-4} pH/s (mean pH_i 6.94 ± 0.07). These results suggest that the Na-H exchangers were unaffected by NBD-Cl.

pH_i Dependency of the H^+ pump fluxes. For experiments in which we monitored the recovery of pH_i in the absence of Na^+ (as in the recovery from the first NH_4^+ pulse in Fig. 11 *A*), we computed total acid-extrusion rates (J_{total}) by multiplying rates of pH_i change by the β_I value prevailing at the appropriate pH_i. The latter was determined from the regression coefficients of the second-order polynomial (Fig. 7 *B*), obtained from experiments on pattern-1 cells. Thus, we have assumed that β_I is the same in pattern-1 and pattern-2 cells. In cells recovering from acute acid loads in the absence of Na^+, J_{total} is the result of fluxes due to the H^+ pump ($J_{H\text{-}ATPase}$) and other acid loading or extrusion processes resistant to NBD-Cl ($J_{NBD\text{-}Cl/R}$). We determined $J_{NBD\text{-}Cl/R}$ values from rates of pH_i change in the eight experiments in which the application of 100 μM NBD-Cl in a Na^+-free solution caused pH_i to

decrease, indicating maximum blockage of the H^+ pumps. The pH_i dependence of $J_{NBD\text{-}Cl/R}$ from these experiments is summarized in Fig. 12 *A* (*inset*), where the negative $J_{NBD\text{-}Cl/R}$ values indicate net acid loading. In the pH_i range 6.9–7.5, $J_{NBD\text{-}Cl/R}$ increased approximately linearly from −25 to −5 μM/s. By subtracting $J_{NBD\text{-}Cl/R}$ from J_{total}, we arrived at $J_{H\text{-}ATPase}$, assuming that the only action of NBD-Cl is to block the H^+ pumps 100%. We calculated $J_{H\text{-}ATPase}$ for 13 cells in which the proton pumps were active in the same pH_i range for which we had β_I values. As shown in Fig. 12 *A*, the magnitude of $J_{H\text{-}ATPase}$, as well as its pH_i dependency, varied considerably from cell to cell. We found H^+ pump activity at pH_i values as low as ~6.75 (Fig. 12 *A*) and as high as ~7.80 (not shown). For all 13 cells, $J_{H\text{-}ATPase}$ decreased with increasing pH_i over at least some range of pH_i values. In three of the 13 cells, $J_{H\text{-}ATPase}$ appears to have an maximal value. As shown in Fig. 12 *B*, the average $J_{H\text{-}ATPase}$ decreased from

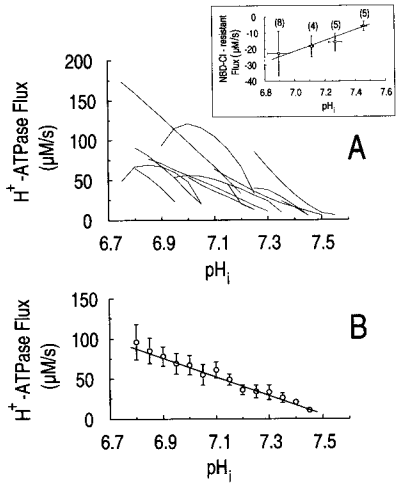

FIGURE 12. pH_i dependence of H^+ pumps. (*A*) Dependence of H^+ pumps fluxes ($J_{H\text{-}ATPase}$), corrected for background acid loading unmasked by 100 μM NBD-Cl ($J_{NBD\text{-}Cl/R}$, the NBD-Cl-resistant flux), on pH_i in 13 separate pattern-2 osteoclasts. (*Inset*) The average relationship of $J_{NBD\text{-}Cl/R}$ vs pH_i. These data were fitted by a straight line with a slope of 34 ± 20 (SD) μM/(s.pH_i) and *y* intercept of −256 ± 144 (SD) μM/s. The number of observations is given in parentheses. Vertical bars represent the SEM, and are omitted if the SEM is not at least 25% greater than the radius of the symbol. (*B*) Average H^+-pump flux vs pH_i relationship. This plot was constructed from the one shown in *A* by averaging at least four data points in a pH_i range. These data were fitted by a straight line with a slope of 117 ± 18 (SD) μM/(s.pH_i) and an intercept of 883 ± 126 (SD) μM/s.

96 to 11 μM/s in the pH_i range 6.8–7.45 in an approximately linear fashion. We found a qualitatively similar dpH_i/dt vs pH_i relationship for seven other cells (not shown) over a more alkaline pH_i range.

DISCUSSION

Overview

To characterize acid-base transporters in osteoclasts, we examined the mechanisms by which freshly isolated rat osteoclasts, plated on glass and studied in the nominal absence of CO_2/HCO_3^-, defend themselves from acute acid loads. Using digital imaging to monitor the fluorescence of BCECF, we found that the cells had a mean initial pH_i of ~7.31 and recovered rapidly from acid loads. In most cells (i.e.,

pattern-1 cells), this recovery was due exclusively to Na-H exchange, which proved to be very sensitive to inhibition by the amiloride analogue HMA. In the remainder of the cells (i.e., pattern-2 cells), which represented a portion of a morphologically distinguishable subgroup of osteoclasts, the pH_i recovery was due at least in part to a Na^+-independent acid extruder that was blocked by NBD-Cl, an inhibitor of vacuolar-type H^+ pumps. In at least some pattern-2 cells, both the Na-H exchanger and the H^+ pump contributed to the pH_i recovery. In addition, we found that the intrinsic intracellular buffering power (β_I) decreased with increasing pH_i values. From the β_I and amiloride data, we deduced that the Na-H exchanger in pattern-1 cells is maximally active at low pH_i values, but is virtually inactive at a pH_i of ~7.1. Finally, H^+ pumps were found active in the pH_i range 6.7–7.8. On average, H^+ pump fluxes tended to decrease with increasing pH_i. Hence, freshly isolated rat osteoclasts express basolateral-type Na-H exchangers, vacuolar-type H^+ pumps, or both, in their plasma membranes.

The Buffering Power of Rat Osteoclasts

The application/withdrawal of weak bases and acids is a common method for determining β_I (Roos and Boron, 1981). The stepwise reduction in $[NH_3]_o$ offers the added advantage of producing the pH_i dependence of β_I, and has been applied in studies of mesangial cells (Boyarsky et al., 1988), gastric parietal cells (Wenzl and Machen, 1989), cardiac Purkinje fibers (Vaughan-Jones and Wu, 1990) and renal epithelial cells (Kraut, Hart, and Nord, 1992). The approach requires that the only mechanism for modulating pH_i be the passive flux of NH_3. Therefore, we conducted our experiments in the nominal absence of Na^+, avoided cells with H^+-pump activity (i.e., pattern-2 cells), and excluded data in which the pH_i drifted more rapidly than 5×10^{-4} pH/s. Removal of Na^+ has been shown not to influence β_I (Vaughan-Jones and Wu 1990; Wilding et al., 1992). In osteoclasts, we found that β_I decreases from ~25 mM at pH_i 6.4 to ~6.0 mM at pH_i 7.3, in a curvilinear fashion (Fig. 7). Thus, the intrinsic buffers are expected to be more effective at defending pH_i from acid than alkali loads. Qualitatively similar β_I-pH_i relationships also are found in the aforementioned cell types. Such β_I-pH_i profiles probably reflect the actions of several intracellular buffers, each with its own pK_a and concentration. However, it is of interest to note that, for rat carotid-body glomus cells, Wilding et al. (1992) were able to approximate their β_I vs pH_i data by assuming the presence of a single intracellular buffer having a pK_a of 6.41 and a total concentration of 41 mM. Using a similar approach, we found that the intracellular buffers of osteoclasts behave as if they were a single buffer with a pK_a of 6.34 and a total buffer concentration of 47 mM.

Evidence for Na-H Exchange in Rat Osteoclasts

Evidence for Na-H exchange in pattern-1 and pattern-2 cells. We defined pattern-1 cells as osteoclasts in which the pH_i recovery from acid loads (Fig. 4) is due exclusively to Na-H exchange. Pattern-1 cells accounted for ~80% of all osteoclasts in our study, and included all cells with extensions and a polygonal and/or elongated shape, as well as ~45% of round cells. We identified Na-H exchange in pattern-1 cells on the basis of two observations: first, the pH_i recovery rate was inhibited ~70% by reducing

$[Na^+]_o$ from 150 to 15.5 mM (Figs. 4 and 5 *B*), and inhibited completely by removing all Na^+ (Figs. 4 *C*, 6 *A*, 7 *A*, and 8 *A*). Second, the pH_i recovery rate was reduced more than 80% by amiloride and by two 5-*N*-substituted amiloride analogues, EIPA and HMA (see Figs. 5 *A*, 6, *B* and *C*, and 8). Pattern-2 cells are those in which pH_i recovered from an acid load in the total absence of Na^+ or in the presence of Na^+ with amiloride. In ~60% of these, the subsequent readdition of external Na^+ led to a substantial increase in pH_i, consistent with the presence of some Na-H exchange activity.

Na-H exchange rates and J_{max} values (Fig. 10) varied widely among osteoclasts. Although it is possible that the explanation for these differences is trivial, such as cell-to-cell differences in cell surface-to-volume ratio, it is intriguing to speculate that the differences reflect the variability in the activity of individual Na-H exchangers or in the surface density of exchangers. It is interesting to note that Na-H exchangers in pattern-2 cells are active at pH_i values that are substantially higher than in pattern-1 cells. For example, Fig. 10 *B* shows that, in almost all pattern-1 cells, Na-H exchange activity approaches zero at a pH_i of 7.1–7.2. On the other hand, Figs. 11 *A* (*inset*) and *C* show that, in pattern-2 cells, Na-H exchange was substantial at pH_i values above 7.3. These observations suggest either that Na-H exchange activity may be regulated by the osteoclast over a wide range, or that pattern-2 cells express a different isoform of the Na-H exchanger. Indeed, our data indicate that H^+ pumps in individual osteoclasts, at least when plated on glass, can be virtually inactive (pattern-1 cells) or extremely robust (pattern-2 cells).

Dependence on pH_i. Fig. 10 summarizes the pH_i dependence of the Na-H exchange rate, corrected for the minor degree of amiloride-insensitive background acid loading that we observed in rat osteoclasts. The two hallmarks of the $J_{Na\text{-}H}$ vs pH_i profile in rat osteoclasts are: (*a*) a rather low $J_{Na\text{-}H}$ near the average initial pH_i, and (*b*) a rather steep dependence of $J_{Na\text{-}H}$ on pH_i as pH_i falls below this initial value. By contrast, in unstimulated UMR-106 cells, an osteoblastic cell line, $J_{Na\text{-}H}$ is fairly high at the initial pH_i and increases only modestly as pH_i falls below this value (Gupta, Schwiening, and Boron, 1994). On the other hand, the pH_i dependence of $J_{Na\text{-}H}$ in UMR-106 cells increases markedly after stimulation with agents such as calcitonin gene-related peptide. The steepness of the $J_{Na\text{-}H}$ vs pH_i relationship can be described by the Hill coefficient (n_H), which averaged 2.9 in our experiments. This suggests that three or more protons interact at the intracellular face of the exchanger, consistent with the presence of an allosteric modifier site (Aronson, Nee, and Suhm, 1982; Aronson, 1985). Although, as noted above, maximal Na-H exchange rates varied two- to threefold from cell to cell, the pH_i values that yielded half-maximal activation of the exchanger ($pH_{1/2}$) fell within a rather narrow range, from 6.64 to 6.78 (Fig. 10 *B*). By analogy with other cells (see, e.g., Grinstein and Rothstein, 1986), one might expect signals from cell surface receptors to affect the pH_i dependency of the osteoclast Na-H exchanger by modulating J_{max}, n_H and/or $pH_{1/2}$.

Inhibition by amiloride and 5-N-substituted amiloride analogues. The Na-H exchangers of osteoclasts were largely blocked by 1 mM amiloride, 50 μM EIPA, or 10–50 μM HMA. In contrast to the blockade produced by amiloride, that produced by EIPA and HMA were poorly reversible, probably reflecting the greater affinity of these two compounds for Na-H exchangers (Kleyman and Cragoe, 1988). The apparent $K_{1/2}$ for

inhibition by amiloride analogues varies widely among Na-H exchangers, though the values generally are far lower for Na-H exchangers in nonepithelial cells and at the basolateral membranes of epithelia than they are for their apical epithelial counterparts (for review see Clark and Limbird, 1991). For example, working with epithelial LLC-PK_1/Cl_4 cells, Haggerty, Agarwal, Reilly, Adelberg, and Slayman (1988) found a $K_{1/2}$ for EIPA of 44 nM for the basolateral, but 13 μM for the apical exchanger. Our value of 49 nM for inhibition of the rat osteoclast Na-H exchanger by HMA in the presence of 150 mM Na^+ is in the range expected for a nonepithelial/basolateral Na-H exchanger.

The paradoxical alkalinization caused by high levels of EIPA or HMA. At concentrations of 50 μM, both EIPA and HMA elicited pH_i increases, even in the absence of Na^+. Conversely, withdrawal of these compounds caused at least a transient decrease in pH_i. Paradoxical alkalinizations induced by 50 μM EIPA also have been observed in NIH-3T3 fibroblasts (Kaplan and Boron, 1994) and rat forebrain astrocytes (Boyarsky, Schlue, Davis, Ransom, and Boron, 1993). At least in the case of HMA, we observed no such paradoxical alkalinization in our osteoclast experiments at concentrations of 10 μM or less. Thus, the effect is restricted to relatively high doses of HMA, doses that are well above those necessary to block the osteoclast Na-H exchanger. As to the mechanism of the alkalinization, our data, and that of others, suggest that it is not due to a dye-HMA interaction. We found that the apparent pH_i increase elicited by 50 μM HMA was paralleled by a reversible decrease in the I_{440} signal, with little change in I_{490}. However, the apparent pH_i (i.e., I_{490}/I_{440}) in osteoclasts is unaffected by 50 μM HMA when we clamped pH_i to 7.00 using a high-K^+/nigericin solution. Moreover, in experiments in which pH_i was monitored with BCECF in mesangial cells (Boyarsky et al., 1988) or renal proximal-tubule cells (Geibel, Giebisch, and Boron, 1989), 50 μM EIPA failed to elicit a paradoxical pH_i increase. Thus, a dye-HMA interaction is an unlikely explanation for the paradoxical pH_i increase. A second explanation is that EIPA and HMA, which are weak bases, enter the cell by nonionic diffusion and become protonated in the cytoplasm. Although there is evidence that the neutral weak-base form of the compounds can indeed enter cells (Kleyman and Cragoe, 1988; Nasri-Sebdami, Cragoe, Cognard, Potreau, and Raymond, 1989), calculations[1] show that equilibration of these weak bases across the membrane would lead to only trivial changes in pH_i. Thus, transport of EIPA or HMA could lead to sizable pH_i increases only if the cell had a mechanism for actively transporting the protonated forms of these amiloride analogues out of the cell. A third explanation for the pH_i increases elicited by EIPA and HMA is that the compounds indirectly produce a change in acid-base transport, or in cellular biochemistry, that would lead to a sustained intracellular alkaline load. Thus, it is

[1] For example, if we assume that the pK_a for HMA is 8.5 (Kleyman and Cragoe, 1988), then at a pH_o of 7.4 and a total HMA concentration of 50 μM, the concentration of the unprotonated, neutral form of HMA would be 3.7 μM. Upon equilibration of this unprotonated HMA across the cell membrane, the intracellular concentration of neutral HMA also would be 3.7 μM. At a pH_i of 6.5, as in Fig. 6 *C*, this 3.7 μM of intracellular neutral HMA would be in equilibrium with 370 μM of protonated HMA, which would have been formed at the expense of 370 μM cytoplasmic H^+. Given an intracellular buffering power of 24 mM/pH at a pH_i of 6.5, this alkali load would have produced a pH_i increase of only 0.015, far less than the alkalinization of ~0.4 shown in Fig. 6 *C*.

likely that, in susceptible cells, high levels of EIPA or HMA produce an increase in pH_i that is real but unexplained.

Evidence for Plasma-Membrane Proton Pumps in Isolated Rat Osteoclasts

Of the round osteoclasts, which lacked cytoplasmic extensions, ~40% (i.e., pattern-2 cells) expressed a Na^+-independent acid-extrusion mechanism that appeared to be an H^+ pump. This conclusion is supported by three observations: first, pH_i recovery from acid loads was brisk, despite the reduction (Fig. 11 *B*) or complete removal of external Na^+ (Fig. 11, *A* and *C*). Second, cells recovered from acid loads in the presence of 1 mM amiloride (Fig. 11 *B*). Finally, the recovery of pH_i from acid loads was blocked rapidly by NBD-Cl (Fig. 11 *C*), an alkylating agent that is rather specific for vacuolar-type H^+ pumps (Blair et al., 1989; for review see Forgac, 1989). Similar criteria have been used by others to infer the presence of plasma-membrane H^+ pumps in macrophages (Bidani, Brown, Heming, Gurich, and Dubose, 1989; Swallow, Grinstein, and Rotstein, 1988, 1990; Tapper and Sundler, 1992).

Osteoclasts are known to alternate between a nonresorbing, migratory phase, in which they exhibit cytoplasmic extensions (lamellipodia), and a resorbing, less motile phase, in which they do not display lamellipodia (Kanehisa and Heersche, 1988; for review, see Teti, Marchisio, and Zambonin-Zallone, 1991) and have a round shape. Several studies indicate that osteoclasts can acidify the bone surface (Baron et al., 1985) and express vacuolar-type H^+ pumps in their ruffled-border membrane during resorption (Blair et al., 1989; Vaananen et al., 1990; Chatterjee et al., 1992). In addition, immunocytochemical studies have shown that osteoclastlike cells generated in vitro stain positively for the vacuolar-type H^+ pump-specific antibody E11 (Kurihara, Gluck, and Roodman, 1990; Wang, Hemken, Menton, and Gluck, 1992). Taken together with these earlier findings, our observation that only 20% of the osteoclasts we studied express functional vacuolar-type H^+ pumps suggests three possibilities. First, only some of the osteoclasts we studied had been involved in bone resorption at the time of isolation. According to this scenario, active osteoclasts would use vacuolar-type H^+ pumps to both resorb bone and regulate pH_i. Nonresorbing osteoclasts, lacking functional H^+ pumps, would use Na-H exchangers to regulate pH_i. Cells in an intermediate state would express both H^+ pumps and Na-H exchangers. The second possibility is that all cells had expressed H^+ pumps in vivo, but most stopped expressing them in their plasma membranes after being plated on glass, where they are not capable of forming a ruffled border. Finally, it is possible that after seeding the osteoclasts on an artificial substratum the H^+ pumps remain inserted in the plasma membrane but are inactivated in the majority of cells. Our data do not address the issue of whether the H^+ pumps we observed were located in a specialized membrane region, as is the case in active cells in situ. Neither do we have direct evidence that the H^+ pumps of freshly isolated osteoclasts are the same as those responsible for bone resorption in vivo.

In conclusion, freshly isolated rat osteoclasts can express two H^+-extruding systems in their plasma membranes: a Na-H exchanger, probably of the ubiquitous basolateral type, and an H^+ pump of the vacuolar type.

This work was supported by NIH grant DK30344 (to W. F. Boron) and DE-04724 and AR-41339 (to R. Baron) and in part by a grant from CIBA-GEIGY (Basel). J. H. Ravesloot was a recipient of a

Brown-Coxe Fellowship and a NATO-Fellowship awarded through the Netherlands Organization for Scientific Research (NWO).

Original version received 1 March 1994 and accepted version received 13 October 1994.

REFERENCES

Aronson, P. S., J. Nee, and M. A. Suhm. 1982. Modifier role of internal H^+ in activating the Na^+/H^+ exchanger in renal microvillus membrane vesicles. *Nature.* 299:161–163.

Aronson, P. S. 1985. Kinetic properties of the plasma membrane Na^+/H^+ exchanger. *Annual Review of Physiology.* 47:545–560.

Baron, R., L. Neff, D. Louvard, and P. J. Courtoy. 1985. Cell-mediated extracellular acidification and bone resorption: evidence for a low pH in resorbing lacunae and localization of a 100 kD lysosomal membrane protein at the osteoclast ruffled border. *Journal of Cell Biology.* 101:2210–2222.

Baron, R., L. Neff, C. Roy, A. Boisvert, and M. Caplan. 1986. Evidence for a high and specific concentration of (Na^+,K^+)ATPase in the plasma membrane of the osteoclast. *Cell.* 46:311–320.

Baron, R. 1989. The molecular mechanisms of bone resorption by the osteoclast. *Anatomical Record.* 224:317–324.

Baron, R., M. Bartkiewicz, M. Chakraborty, D. Chatterjee, C. Fabricant, N. Hernando, W. C. Horne, A. Lomri, L. Neff, J.-H. Ravesloot, and Y. Su. 1992. Ion transport and the molecular mechanisms of bone resorption. *In* Calcium Regulating Hormones and Bone Metabolism. D. V. Cohn, C. Gennari, and A. H. Tashjian, Jr, editors. Elsevier, Amsterdam. 131–141.

Bidani, A., S. E. S. Brown, T. A. Heming, R. Gurich, and T. D. Dubose, Jr. 1989. Cytoplasmic pH in pulmonary macrophages: recovery from acid load is Na^+ independent and NEM sensitive. *American Journal of Physiology.* 257:C65–C76.

Blair, H. C., S. L. Teitelbaum, R. Ghiselli, and S. Gluck. 1989. Osteoclastic bone resorption by a polarized vacuolar proton pump. *Science.* 245:855–857.

Boron, W. F. 1983. Transport of H^+ and of ionic weak acids and bases. *Journal of Membrane Biology.* 72:1–16.

Boyarsky, G., M. B. Ganz, R. B. Sterzel, and W. F. Boron. 1988. pH regulation in single glomerular mesangial cells. I. Acid extrusion in absence and presence of HCO_3^-. *American Journal of Physiology.* 255:C844–C856.

Boyarsky, G., W.-R. Schlue, M. B. E. Davis, B. Ransom, and W. F. Boron. 1993. Intracellular pH regulation in single cultured astrocytes from rat forebrain. *Glia.* 8:241–248.

Boyde, A., N. N. Ali, and S. L. Jones. 1984. Resorption of dentine by isolated osteoclasts in vitro. *British Dental Journal.* 156:216–220.

Chaillet, J. R., and W. F. Boron. 1985. Intracellular calibration of a pH-sensitive dye in isolated perfused salamander proximal tubules. *Journal of General Physiology.* 86:765–794.

Chambers, T. J., P. A. Reveli, K. Fuller, and N. A. Athanasou. 1984. Resorption of bone by isolated rabbit osteoclasts. *Journal of Cell Science.* 66:383–399.

Chatterjee, D., M. Chakraborty, M. Leit, L. Neff, S. Jamsa-Kellokumpu, R. Fuchs, and R. Baron. 1992. Sensitivity to vanadate and isoforms of subunits A and B distinguish the osteoclast proton pump from other vacuolar H^+ ATPases. *Proceedings of the National Academy of Sciences USA.* 89:6257–6261.

Clark, J. D., and L. E. Limbird. 1991. Na^+-H^+ exchanger subtypes: a predictive review. *American Journal of Physiology.* 261:C945–C953.

Eisen, T., Y. Su, R. Baron, and W. F. Boron. 1991. The regulation of intracellular pH in rat osteoclasts studied in the absence of HCO_3^-. *Journal of Bone and Mineral Research.* 6(Suppl.):53*a*. (Abstr.)

Forgac, M. 1989. Structure and function of vacuolar class of ATP-driven proton pumps. *Physiological Reviews.* 69:765–798.

Gay, C. V., M. B. Ito, and H. Schraer. 1983. Carbonic anhydrase activity in isolated osteoclasts. *Metabolism, Bone Disease, & Related Research.* 5:33–39.

Geibel, J., G. Giebisch, and W. F. Boron. 1989. Basolateral sodium-coupled acid-base transport mechanisms of the rabbit proximal tubule. *American Journal of Physiology.* 257:F790–F797.

Green, J., D. T. Yamaguchi, C. R. Kleeman, S. Muallem. 1988. Cytoplasmic pH regulation in osteoblasts. Interaction of Na^+ and H^+ with the extracellular and intracellular faces of the Na^+/H^+ exchanger. *Journal of General Physiology.* 92:239–261.

Grinstein, S., S. Cohen, and A. Rothstein. 1984. Cytoplasmic pH regulation in thymic lymphocytes by an amiloride-sensitive Na^+/H^+ antiport. *Journal of General Physiology.* 83:341–369.

Grinstein, S., and A. Rothstein. 1986. Mechanisms of regulation of the Na^+/H^+ exchanger. *Journal of Membrane Biology.* 90:1–12.

Gupta, A., C. J. Schwiening, and W. F. Boron. 1994. Effects of CGRP, forskolin, PMA and ionomycin on the pH_i dependence of the Na-H exchanger in UMR-106 cells. *American Journal of Physiology.* 266:C1083–C1092.

Haggerty, J. G., N. Agarwal, R. F. Reilly, E. A. Adelberg, C. W. Slayman. 1988. Pharmacologically different Na/H antiporters on the apical and basolateral surfaces of cultured porcine kidney cells (LLC-PK1). *Proceedings of the National Academy of Sciences, USA.* 85:6797–6801.

Hall, T. J., and T. J. Chambers. 1989. Optimal bone resorption by isolated rat osteoclasts requires chloride/bicarbonate exchange. *Calcified Tissue International.* 45:378–380.

Hall, T. J., and T. J. Chambers. 1990. Na^+/H^+ antiporter is the primary proton transport system used by osteoclasts during bone resorption. *Journal of Cell Physiology.* 142:420–424.

Kanehisa, J., and J. N. M. Heersche. 1988. Osteoclastic bone resorption: in vitro analysis of the rate of resorption and migration of individual osteoclasts. *Bone.* 9:73–79.

Kaplan, D. L., and W. F. Boron. 1994. Long-term expression of c-H-*ras* stimulates Na-H and Na^+-dependent Cl-HCO_3 exchange in NIH-3T3 fibroblasts. *Journal of Biological Chemistry.* 269: 4116–4124.

Kleyman, T. R., and E. J. Cragoe, Jr. 1988. Amiloride and its analogs as tools in the study of ion transport. *Journal of Membrane Biology.* 105:1–21.

Kraut, J. A., D. Hart, and E. P. Nord. 1992. Basolateral Na^+-independent Cl^--HCO_3^- exchange in primary cultures of rat IMCD cell. *American Journal of Physiology.* 263:F401–F410.

Kurihara, N., S. Gluck, and G. D. Roodman. 1990. Sequential expression of phenotype markers for osteoclasts during differentiation of precursors for multinucleated cells formed in long term human marrow cultures. *Endocrinology.* 127:3215–3221.

Nasri-Sebdani, M., E. J. Cragoe, Jr., C. Cognard, D. Potreau, and G. Raymond. 1989. The depressant effects of some amiloride analogues on the slow outward K^+ current and contraction of voltage-clamped frog fibres. *European Journal of Pharmacology.* 171:97–107.

Paradiso, A. M. 1992. Identification of Na^+-H^+ exchange in human normal and cystic fibrotic ciliated airway epithelium. *American Journal of Physiology.* 262:L757–L764.

Raley-Susman, K. M., E. J. Cragoe, Jr., R. M. Sapolsky, and R. R. Kopito. 1991. Regulation of intracellular pH in cultured hippocampal neurons by an amiloride-insensitive Na^+/H^+ exchanger. *Journal of Biological Chemistry.* 266:2739–2745.

Ravesloot, J. H., W. F. Boron, and R. Baron. 1992. Proton extrusion in osteoclasts can occur via a basolateral-type Na^+/H^+ exchanger or via a Na^+ independent, amiloride-insensitive H^+ extruder. *Journal of Bone and Mineral Research.* 7(Suppl.):150*a*. (Abstr.)

Roos, A., and W. F. Boron. 1981. Intracellular pH. *Physiological Reviews.* 61:296–434.

Schwiening, C. J., and W. F. Boron. 1994. Intracellular pH regulation in CA1 neurones freshly

isolated from rat hippocampus: Role of Na^+-dependent transporters. *Journal of Physiology.* 475:59–67.

Swallow, C. J., S. Grinstein, and O. D. Rotstein. 1988. Cytoplasmic pH regulation in macrophages by an ATP-dependent and *N,N'*-dicyclohexylcarbodiimide-sensitive mechanism. *Journal of Biological Chemistry.* 263:19558–19563.

Swallow, C. J., S. Grinstein, and O. D. Rotstein. 1990. A vacuolar type H^+-ATPase regulates cytoplasmic pH in murine macrophages. *Journal of Biological Chemistry.* 265:7645–7654.

Tapper, H., and R. Sundler. 1992. Cytosolic pH regulation in mouse macrophages. Proton extrusion by plasma membrane localized H^+-ATPase. *Biochemical Journal.* 281:245–250.

Teti, A., P. C. Marchisio, and A. Zambonin-Zallone. 1991. Clear zone in osteoclast function: role of podosomes in regulation of bone-resorbing activity. *American Journal of Physiology.* 261:C1–C7.

Teti, A., H. C. Blair, S. L. Teitelbaum, A. J. Kahn, C. Koziol, J. Konsek, A. Zambonin-Zallone, and P. H. Schlesinger. 1989. Cytoplasmic pH regulation and chloride/bicarbonate exchange in avian osteoclasts. *Journal of Clinical Investigation.* 83:227–233.

Thomas, J. A., R. N. Buschbaum, A. Zimniak, and E. Racker. 1979. Intracellular pH measurements in Ehrlich ascites tumor cells utilizing spectroscopic probes generated in situ. *Biochemistry.* 81:2210–2218.

Vaananen, H. K., E. K. Karhukorpi, K. Sundquist, B. Wallmark, I. Roininen, T. Hentunen, J. Tuukkanen, and P. Lakkakorpi. 1990. Evidence for the presence of a proton pump of the vacuolar H^+-ATPase type in the ruffled border of osteoclasts. *Journal of Cell Biology.* 111:1305–1311.

Vaughan-Jones, R. D., and M.-L. Wu. 1990. pH dependence of intrinsic H^+ buffering power in the sheep cardiac Purkinje fibre. *Journal of Physiology.* 425:429–448.

Wang, Z. Q., P. Hemken, D. Menton, and S. Gluck. 1992. Expression of vacuolar H^+ ATPase in mouse osteoclasts during in vitro differentiation. *American Journal of Physiology.* 263:F277–F283.

Wenzl, E., and T. E. Machen. 1989. Intracellular pH dependence of buffer capacity and anion exchange in the parietal cell. *American Journal of Physiology.* 257:G741–G747.

Wilding, T. J., B. Cheng, and A. Roos. 1992. pH regulation in adult rat carotid body glomus cells. Importance of extracellular pH, sodium and potassium. *Journal of General Physiology.* 100:593–608.